Unterschrift des Betreuers

TU WIEN

TECHNISCHE UNIVERSITÄT WIEN

D I P L O M A R B E I T

Physical characterization and rapid prototyping of functional biomedical adhesives for membrane- and electrode-integrated cell-based lab-on-a-chip systems

———————————————————————————
Thema

Ausgeführt am Institut für

E163 Institut für Angewandte Synthesechemie
E164 Institut für Chemische Technologien und Analytik

———————————————————————————
der Technischen Universität Wien

Univ. Prof. Dipl.-Ing. Dr. Peter Ertl
unter der Anleitung von **Dr.nat.techn., MSc Mario Rothbauer** _____

durch

B.Sc. Sebastian Kratz

———————————————————————————
Name

Rueppgasse 11/3a in 1020 Wien

———————————————————————————
Anschrift

_____   _____
10.01.2018
Datum   Unterschrift (Student)

Physical characterization and rapid prototyping of functional biomedical adhesives for membrane- and electrode-integrated cell-based lab-on-a-chip systems

Master Thesis

Author: Sebastian Kratz

First Supervisor: Univ. Prof. Dipl.-Ing. Dr. Peter Ertl

Second Supervisor: Dr.nat.techn., MSc Mario Rothbauer

January 2018, Vienna

Vienna University of Technology
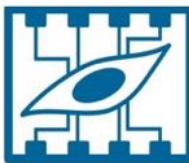
Faculty of Technical Chemistry

Institute for Applied Synthetic Chemistry & Institute for Chemical Technologies and Analytics

Cell Chip Group

"*Everything not saved will be lost.*" – Nintendo "Quit Screen" message

Preface

This study establishes a method for rapid prototyping of membrane- and electrode-integrated cell-based lab-on-a-chip systems to study the barrier function of the placenta. There is still an urgent need to better understand the functions of the human body and its organs. The motivation is to create better clinical models to improve the quality of life and reducing animal testing for pharmaceutical studies.

Acknowledgments

It wouldn't have been possible for me to conduct this study without the support of several people. I would especially like to thank my supervisor Dr. Mario Rothbauer and as well Univ. Prof. Dipl.-Ing. Dr. Peter Ertl for their generous support, coaching and introducing me to the field of microfluidic and lab-on-chip technologies. They shared their expertise very generously with me and I have learned a lot from them.

As well I would like to thank the whole cell chip group who have always had time for my questions and to support me with helpful answers. Beside the shared expertise every shared, coffee, beer or banana talk was a pleasure. Thank you all for being part of my work to achieve my diploma.

Contents

1 Abstract

To gain progress in medicine and drug research the human body has to be understood as precise as possible. The human body is made up of various organs. Each organ has representative functional units. In regards of those units the pathology and drug uptake has to be understand. The widely spread method to either static culture cells of those functional units or conduct animal trials are quite unsatisfactory. Beside the major lack in the transferability of animal models, it is ethical questionable to conduct animal trials. Static cultivation has the disadvantage to not mimic the physiological microenvironment inside the tissue.

This gap is closed by cultivating cells in a perfused lab-on-a-chip system which mimics the microenvironment of the tissue. With this technology cell are dynamically cultured with defined parameters regarding: topographical guidance, mechanical stimuli and biochemical gradients as well as cell to cell interaction, tissue to tissue interfaces, cell morphologies and biomechanics. By engineering those factors and integrating electrical sensors to enhance the read out of this microenvironment, a dynamic complex model of an organ or the functional unit of it can be created.

The placenta develops during pregnancy to support the growing child with functions essential for survival, like oxygen and nutrients supply. This exchange between the maternal and the fetal blood circuit happens a the microvilli, the functional unit of the placenta. There syncytiotrophoblast are exposed to the maternal blood. The syncytiotrophoblast build up a paracellular barrier where the cells are fixed to each other by tight junctions.

The placenta barrier is remodeled by creating a membrane integrated cell based lab-on-a-chip system. Here two microfluidic channels are separated by porous polyester membrane. BeWo b30 cells, derived from a human placenta choriocarcinoma are cultured on this membrane to model the placenta barrier between the maternal blood as the upper channel and the fetal blood as the lower channel. The key parameter, the tightness of the barrier, is observed by measuring the establishment of tight junctions. By integrating electrodes in the membrane integrated cell based lab-on-a-chip system the trans-epithelial electrical resistance can be measured during the experiment. The increase of the resistance over the epithelial membrane is directly linked to the formation of tight junctions.

To conduct a proper experiment a interface is designed and tested for 4 weeks. The interface ensures an easy and leakage free connection of the chip to the lab environment.

The engineering of the membrane- and electrode-integrated cell-based lab-on-a-chip system is carried out by using functional biomedical adhesives. The advantage of the pressure sensitive double-sided adhesive tapes is, that they only require a one-step manufacturing (cutting) which results in a superior short time for concept-to-chip. Pressure sensitive double-sided adhesive tapes offer rapid prototyping with in less than one hour. Because they have an already incorporated biocompatible adhesive layer they can easily bonded to glass and membranes by applying pressure. This very fast bonding procedure reduces the time for concept-to-chip radically.

To choose the best pressure sensitive double-sided adhesive tape out of ARcare 92712, ARcare 90445, ARcare 90106 and ARseal 90880, the tapes are physically characterized in regards of the tolerance of the cut structures, level of barrier to vapor, hydrophilicity of the adhesive layers and the highest bonding strength to the membranes. To ensure proper cell culturing in the chip, cell compatibility as well as cell viability is studied.

ARcare 90445 shows the smallest tolerance, no vapor rate, the highest hydrophilicity, the highest bonding strength to membranes and the best cell compatibility as well as as negligible influence on the cell viability. Further more the optical properties give no further restrictions.

Powder blasting is conducted and used to create higher channel structures and connection holes through glass.

The membrane- and electrode-integrated cell-based lab-on-a-chip system is manufactured within 3h and to proof the evidence of the lab-on-a-chip system TEER measurement with BeWo b30 cells are carried out over 7 days. The influence of the trans-epithelial electrical resistance by the cells is proven through trypsin which detaches the cells from the membrane. A functional membrane- and electrode-integrated cell-based lab-on-a-chip system is established.

2 Introduction

2.1 Cell-based lab-on-a-chip systems

Understanding and modeling the human physiology is of key interest in clinical and medical research. Beside understanding the human organism as a whole, an understanding of each functional element, the organs, is necessary as well. Every organ supports the human organism with different functions. Therefore, every organ can be modeled as an interaction of multiple functional units.

With regards to medical and drug research two main aspects are important: basic understanding of organ function in health and disease as well as predicting uptake and metabolism of drugs [1].

Such insights can be gained either by studying tissue samples and cells with bottom up approach or as a top down strategy applying animal models. Biggest issue of both approaches is the lack transferability to human organism physiology. On the one hand, *in vitro* cultures of human cells and tissue samples do feature human physiology to some extant, however, they lack correct boundary conditions. Under classical static two-dimensional cultivation the cells are excluded from their natural and highly dynamic microenvironment, which severely influences cellular behavior. This can even lead to wrong assumption [2].

Animal models on the other hand represent the most complex model available and provide insights into physiology and pathophysiology in the context of a whole living organism. Because of species specific differences in physiology on an organism level, animal models can only model specific key functions of organs rather than a whole organism and must be selected accordingly [3, 4, 5]. In particular 90% of the genome of mouse and human is identical and therefore a suitable model to remodel the human organism as a whole [6]. Guinea pigs as an animal model can remodel specific functions of the human lipoprotein metabolism [7]. Depending on the level of remodeling the organ, for example the placenta, the remodeled key factor differ from species to species. Human and sheep have the same placenta structure as villous but differ drastically in the placenta shape [8]. For example it is estimated that only 8% of the successfully conducted animal trials of cancer drugs can be transferred to successful human application [9].

Nowadays it costs up to 2.5 billion dollars and takes a period of 10-12 years on average to bring a clinically applicable drug to the market, where two thirds are spent in the clinical trial stage [3, 10]. Beside the vast cost driving factors to bring a pharmaceutical product from the bench to the bed of the patient, animal testing is ethical questionable. Due to the consumption of test animals.

To close the gap between those well established model systems and human physiology, the complexity especially of *in vitro* static models applying static culture conditions in plastic petri dishes need to be increased by using novel and *in vivo*-relevant culture tools and techniques such as three-dimensional culture and perfused bioreactors [11].

On the one hand the biophysical properties have to be engineered through bioreactors, mechanical bioreactors and microfluidic as topographical guidance, mechanical stimuli and biochemical gradients to establishing a dynamic micro environment for a good organ model [12]. Especially microfluidic is a promising technology because sample size is in range of microliter which reduces the amount of needed chemicals, reagents or drugs to a minimum [13]. On the other hand the biological considerations deal with cell morphology and phenotype, direct and indirect cell-to-cell interaction as well as tissue architecture [1].

Beside using those technologies to mimic the microenvironment it is also necessary to measure and regulate the parameters of this dynamic system. The quantification and validation of these advanced culture models is a technological challenge due to invasiveness of most analytical techniques. Frequently the choice is either employ dyes and essays that may change the biology or to use end-point detection means [14, 15]. Here, the application non-invasive optical, magnetic, chemical, electrical and electrochemical biosensors is of great potential [16].
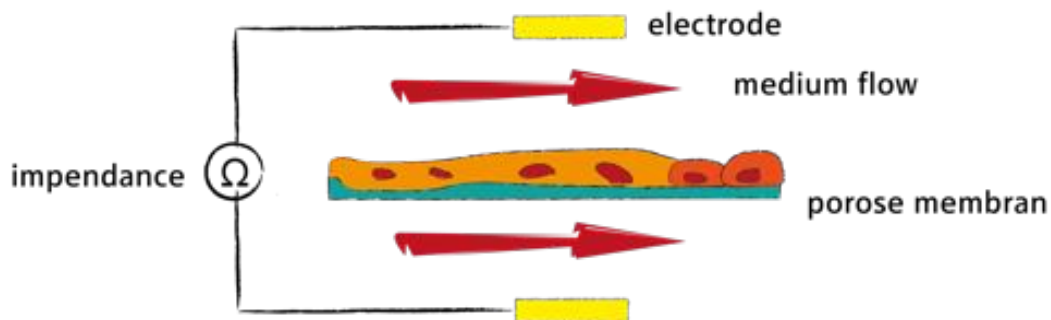
Figure 1: Principle of Trans-epithelial electrical resistance

Trans-epithelial electrical resistance (TEER) is used to characterize the quality of the barrier function of epithelial and endothelial cell monolayers by measuring the impedance across those (see Figure 1). The big advantage of TEER by applying a current across the barrier is that it is a non-destructive, label free method, providing real-time information on the barrier quality. This gives a strong tool to have real time quantification of the quality of the barrier within a membrane-integrated cell based lab-on-a-chip. The principles is that there are two pathways for ion transport across the cell monolayer: 1) the transcellular pathway, which includes lipophilic, receptor-mediated, adsorptive and protein transport, and 2) the paracellular route that involves transport through cell tight junctions and the intercellular space [17]. The corresponding circuit model is where transported ions and other charged molecules are the charge carriers in the system. The transcellular pathway is the sum of all apical cell membrane resistance and the basolateral cell membrane resistance. The paracellular pathway is equal to the sum of the tight junction resistance and the intercellular resistance [17]. In the beginning the paracellular pathway dominants the TEER measurement when adherent junctions or tight junctions between the cells have not yet formed [17]. Later on the TEER measurement is related to the electrical impedance across an epithelium or endothelium because to the formation of robust tight junctions between neighboring cells. Beside as a well established method for static transwell cell cultivation TEER measurements on perfused chips is quite a challenging task [18].

The combination of biosensors with microfluidic is called "lab-on-a-chip". Human cells cultured in a lab-on-chip leads to broader and more precise readout of the dynamics. It is a dynamic system, mimicking the microenvironment through microfluidic for specific tissue with integrated sensors in a size of a common computer chip. Those devices help to understand the human organ's fundamental microarchitectures and functions.

It can be distinguish between three main concepts of to model the human organism on different levels. For modeling the a functional unit within a organ, parenchymal tissue on a chip (I) are defined, for modeling an interface between two functional units, tissue interface on a chip (II) are defined and for modeling more than on organ on a chip body on a chip (III) is defined [1].

To establish models as close as possible to the human organism there is still a need of new material and manufacturing methods to hit the complexity of a human organ with a lab-on-a-chip.

2.2 Engineering a cell-based lab-on-a-chip system
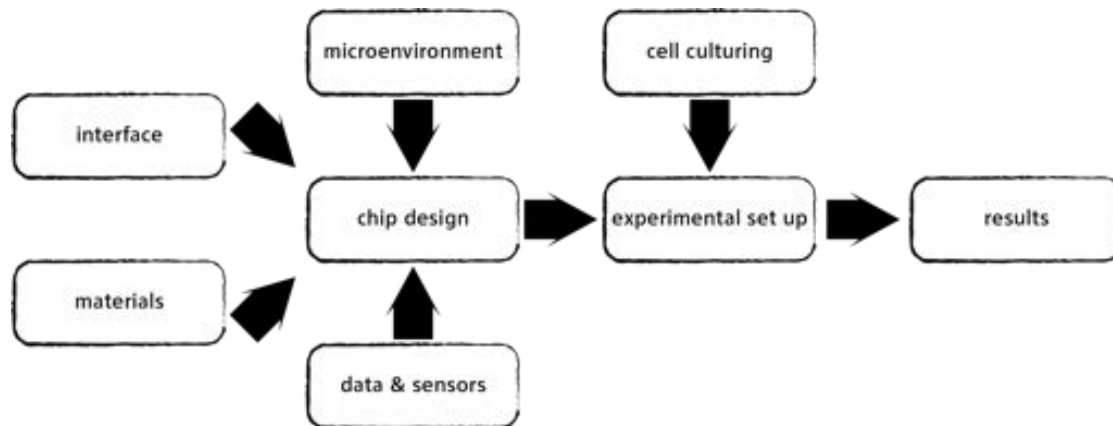
Figure 2: Developing and engineering a cell-based lab-on-a-chip systems

To create more complex models of the human organs a set of different design and engineering steps have to be considered (see Figure 2): the interface, the materials, the bioengineering, the sensors and read out which all influence the chip design and there for the physical microenvironment. The chip combined with the cell model (biochemical microenvironment) make up the experimental set up and leads to results [19].

Of course most of these steps are highly depending on the organ and the function which should be modeled. The organ and its functional unit defines the guidelines for the microenvironment and the mimicking of it within the chip. There are two approaches: one possibility is that the chip itself mimics the functions unit of the organ or that the cells in the chip represents the functional unit. Both requires different materials with different specifications which comes a long with restrictions for the engineering process.

Figure 3: A) schematic drawing of lung-on-a-chip (taken from ref. [20]) B) schematic drawing of liver-on-a-chip (taken from ref. [21])

For example to model the lung and its functions unit alveoles: a epithelial-endothelial interface, a epithelial-air interface, a endothelium-blood interface are needed which results in a dynamic mechanical membrane system (see Figure 3 A) [22]. Here the chip mimics the expanding of the aveoles by stretching the membrane by applying a vacuum. Another ex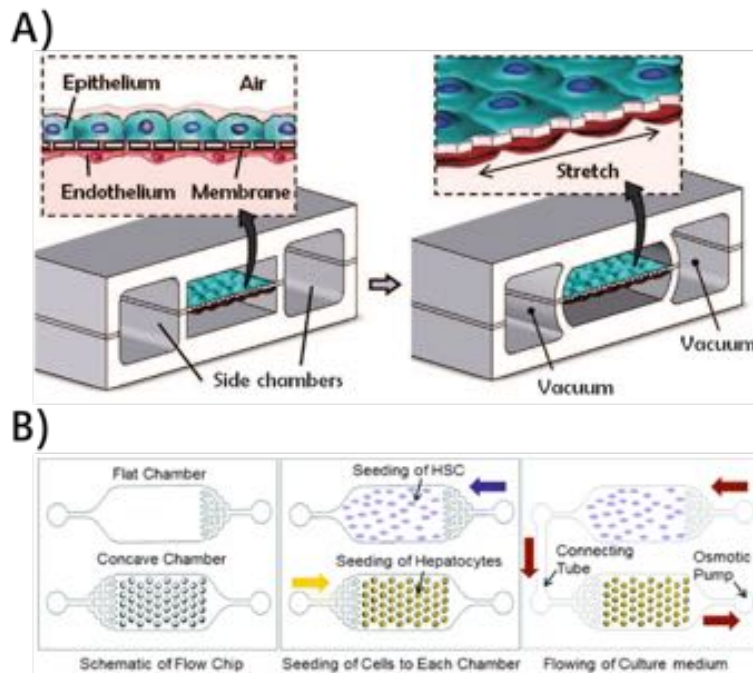ample is to model the liver as an organ as a whole with help of organoids with in a chip (see Figure 3 A)[23]. Here the cells as organoids with their metabolism represent the functional unit.

First the physiological microenvironment of the specific tissue or organ is defined and afterwards rebuild in the lab-on-a-chip. Secondly the isolated homologous tissue cells are stimulated by bimolecular gradients, flow-induced shear stress and mechanical strain, while nutrients are transported by microfluidics [19]. Thirdly it should give insights for basic science and clinical studies by showing physiological relevance and the capability to reflect key properties of *in vivo* scenarios and functions of the organs. Beside those academic factors a cell-based lab-on-a-chip systems should be robust and have a facilitate standardization and a high throughput [11].

To put a microenvironment into practice a set of suitable materials is needed. The materials have to be manufacturable on the one hand and biocompatible on the other hand. The way signals (optical, electrical etc.) are recorded influences the choice of materials as well. To maintain the microenvironment, to support the cells in culture and access the data a proper interface is needed. All these factors determine the chip design.

When the chip is combined with the right cell line of the representing organ unit the experiment set up can be established to observe either pathological behavior or responds to drugs. The advantage is that micro engineered physiological models with self-organizing tissues can be taken as more realistic functional and representative human organ model. Cell-based lab-on-a-chip systems displaying physiology better than tissues cultured in conventional systems [19].

11

2.2.1 Organ models in lab-on-a-chip systems

Micro engineered Physiological Systems	Organ-on-a-chip	Key organ function	Specific requirements
Anatomically Inspired Organ Function Mimicking	Arteries-on-a-Chip	regulate the flow and redistribution of blood in organs	loading, precise placement, fixation as well as controlled perfusion and superfusion of a fragile resistance artery segment
	Spleen-on-a-Chip	blood surveillance	physiological flow division to mimic the closed-fast and the open-slow microcirculations
Membrane-Based Penetration and Mechanical Stimuli	Blood–Brain Barrier	selective barrier	Microenggneering membranes with small thickness, high porosity, and regular pores distribution
	Kidney-on-a-Chip	full filtration and reabsorption behaviors	two microfabricated layers separated by a porous membrane
	Lung-on-a-Chip	gas exchange	Fluid and solid mechanical stresses through stretchable membrane
	Gut-on-a-Chip	absorption of drugs and nutrients	including cyclic mechanical strain, fluid flow
	Heart-on-a-Chip	contractility of cells to pump blood	observe the contractility of muscle tissue by electrodes
Perfusion-Based Microenvironments and Functional Culture	Liver-on-a-Chip	metabolism	perfused culturuing compartments for spheroids

Table 1: Organ models in lab-on-a-chip systems (taken from ref. [19])

As Table 1 shows every key organ function which needs to be modeled comes a long with specific requirements for the chip functions. The key function of the organ can be the metabolism of the tissue, mechanical behavior or the exchange of substances. The chip function reaches from separating several chambers by porous membranes up to cyclic mechanical strain in the lab-on-a-chip.

In this study the placenta barrier is chosen as a membrane model. The main function of the placenta is to enable a selected nutrient and gas exchange on the one hand and to physical separate between the mothers blood circuit and the the fetal blood circuit on the other hand [24]. Therefore the basic design approach is to establish a working membrane-integrated cell-based lab-on-a-chip system. To observe the barrier tightness the membrane trans-epithelial electrical resistance (TEER) is measured by integrating electrodes on the membrane-integrated cell-based lab-on-a-chip system.

2.2.2 Placenta as a membrane model

The placenta is a organ which develops due to fertilization within the female human body to maintain the pregnancy[25, 26]. The key function of the placenta is to mediate the exchange of different endogenous and exogenous substances and gases between the mother and fetus during pregnancy [27].
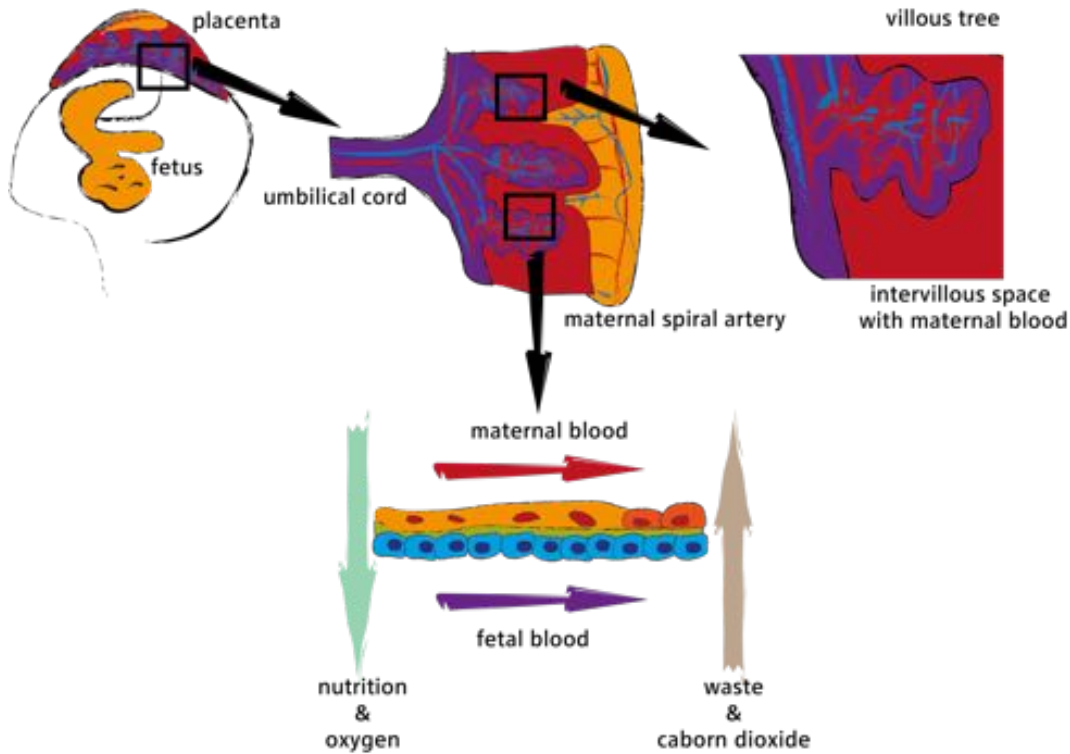

Figure 4: Placenta barrier as a membrane model: the fetus connected to the placenta by the umbilical cord; the intervillous space between the mothers blood circuit and the the fetal blood circuit; the villous trees and the schema of the placenta barrier as a membrane model

During the first trimester of the pregnancy cell from the placenta and the fetal extravillous trophoblast invading the uterine wall directly in a controlled way. Those cells rebuild the spiral arteries into highly dilated vessels for providing sufficient nutrients and oxygen to the fetus[28]. Those remodeled structures are called the villous tree (see Figure 4) which are composed of villous syncytiotrophoblast, villous cytotrophoblasts as well as placental endothelial cells. The villous syncytiotrophoblast represent the outer layer, a epithelia with absence of lateral cell borders and the establishment of tight junctions [29].

Beside maintaining the gas transfer for the fetus and therefore replacing the lung, the exchange of catabolic substance as well as the resorption of those instead of the gut, the placenta replaces a batch of vital function. The placenta regulates a lot of excretory functions as the water balance and the ph regulation instead of the kidney as well as the syntheses and secretion instead of most of the endocrine glands. To replace the function of the liver numerous metabolic substances are released by the placenta for the fetus. In the early pregnancy the placenta supports the formation of bone marrow as well. Further more the placenta controls the heat transfer for the fetus instead of the skin air interface and still largely unknown supports immunological functions [8].

Next to the passive transport by diffusion of gasses and water, depending of the thickness of the placenta barrier, all other substances are transporter active by the surface. This is managed by carrier molecules (glucose) , enzymes (amino acids and ions) and receptors for vesicle transport (peptides, proteins and lipids) [8].

In case of a shortage of the oxygen supply (hypoxia) in the placenta two main problems will arise: first of all the fetus will suffer from under-supply of oxygen and the placenta cells (cytotrophoblasts) will be harmed [30].

Hypoxia, oxidative stress and high blood pressure can cause a preeclamptic placenta, a pathological development. Preeclampsia, affecting 5%–8% of pregnancies, is one of the major contributors of maternal and perinatal morbidity and mortality [31].

Nowadays the environment is polluted by artificial nanoparticles which can enter the maternal blood circuit and causes harm for the fetus [32]. In regards of drug research the placenta can be an aim to drugs or through the active transport properties the placenta barrier interferes with drug delivery to the fetus as well as xenobiotic metabolism enzymes.

Furthermore through the tools of different disciplines like mathematics and mechanics, organs can be understood in a more physical way which eases the modeling of the microenvironment. For example the blood flow with in the placenta can be simulated to understand the causes of high blood pressure. This scenario can be established on cell-based lab-on-a-chip system as well by different flow and pressure scenarios [33, 34]. By understanding the flow conditions in the placenta it is also possible to model the fluidic force in the intervillous space and defining different scenarios with different shear force on the cell layer [33, 35]. Through the progress of medical imaging technics like micro computertomography the three dimensional structures of organs as the placenta can be described and remodel by surface or volume ratio [36]. Those insights are the base to mimic the microenvironment for the placenta as a membrane- and electrode-integrated cell-based lab-on-a-chip systems.

2.3   Micro fabrication materials and techniques for lab-on-a-chip systems

To model the placenta and the crucial functional unit, the placenta barrier, a membrane-integrated cell-based lab-on-a-chip is needed. The technical challenge is to generate and control the physiological structure. This designing process goes a long with a trade off between complexity, which improves its physiological relevance and its practical operation and management [37]. Therefore a two channel system separated by a membrane must be established.

Nowadays chips are mostly produced out of Polydimethylsiloxan (PDMS), a biocompatible silicone which can be cured with structures down to 20 µm [11, 19, 22, 23, 38, 18]. Beside the vast application of PDMS in research in individual chip designs, there is still a lack of fast scale technics. PDMS is generally manufactured through replication by casting structures within molds [39].

For a large scale production two industrial replication technics as hot embossing and injection molding are important. For small scale production, in a research environment for example, a quick and simple fabrication is important. By shortening the concept-to-chip time research progress in regards of evaluating the influence of specific features on the performance of the overall system can be increased. Casting of PDMS by molds require the creation of a replication master for creating the microfluidic structure only in the second process step—they can therefore be termed two-(or multi-)step manufacturing techniques[40]. In many cases the number of pieces of a needed design is very low, sometimes a low as one. Therefore every one-step manufacturing where a microfluidic structure can be directly produces from a digital three-dimensional model give a enormous reduction in concept-to-chip times and eases the improvement of the chip design by iterating steps. One-step manufacturing can bring advantages to manufacturing cost, industrial manufacturability and hit the need of standardization of the production [41].

With this time very low, working with out replication techniques (which require the creation of a replication tool) and create structures directly without intermediated steps it is really possible to have rapid prototyping [40].

To avoid the time consuming procedure to mix and cast structures within molds, PDMS can also purchased as a foil and then cut down to 300 µm small structures and then used as a layer for chip production. Cutting plotter is a an easy rapid tool to produce structures in scale of hundreds of micrometers from a computer-generated layout. The big advantage compared to laser cutting of those materials is that there are no residual waste products from the burning process[42]. The simple cutting technic provides an easy, clean-room free way for rapid prototyping and a very short concept-to-chip time [1]. The same technic can be used to machine biocompatible pressure sensitive double-sided adhesive tapes. They come with the advantage that they are quite cheap and have already an incorporated adhesive layer which eases the bonding to glass and membranes a lot compared to PDMS [43]. To build chips with those tapes, they are cut and squeezed together with the other materials as membranes and glass with integrated electrodes. They enable rapid prototyping with only one step manufacturing and a superior short concept-to-chip time. The are originally suggested for bonding, laminating and assembly of in-vitro diagnostic and related membrane-based immunoassay products. Their defined hight determines the hight of the structure which is a design restriction.

In general the one-step techniques can be distinct in material removing techniques and material depositing techniques (see table 2). The material removing techniques as electrical discharge machining, laser direct machining, etching and mechanical structuring is taken to manufacture structures with a resolution of several µm in polymers, metals, ceramics and glass. For manufacturing structures by depositing silicon, polymers, photoresists and hydrogels silicon surface micro machining, lithography and 3D printing with a resolution of several µm is used.

Glass, beside PDMS is a very common material for lab-on-a-chip devices. Glass is biocompatible, robust, chemically-stable, has very good optical properties and can be used to reproduce microfluidic structures having high-resolution integrated electrodes and/or active sensing elements. The main problem with glass is the machining (etching) of it and the bonding of the machined parts. This steps requires cleanroom conditions to avoid dust particles affecting the yield, specialized tools, and high temperature bonding or annealing steps (typically above 500 °C) [42]. There for in this study glass is machined with powder blasting and bonded by pressure sensitive double-sided adhesive tapes.

15

Material removing techniques						
Process	**Lateral size**	**Reso-lution**	**Materials**	**Cost/ piece**	**Time/ piece**	**Channel bonding required**
Electrical discharge machining	µm–cm	25 µm	Polymers, metals, ceramics	High	Low	Yes
Laser direct machining	µm–m	several 100 µm	Polymers, metals, ceramics	Low	Low	Yes
Etching	µm–mm	sub µm–cm	Polymers, metals, glass, silicon	Low	Medium	Yes
Mechanical structuring	mm–cm	20 µm–cm	Polymers, metals, glass, ceramics	Medium	High	Yes
Material depositing techniques						
Process	**Lateral size**	**Reso-lution**	**Materials**	**Cost/ piece**	**Time/ piece**	**Channel bonding required**
Silicon surface micro machining	µm–cm	sub µm–cm	Silicon, silicon nitride, silicon oxide	Medium	Medium	Yes
Lithography	mm–cm	Sub µm–cm	Photoresists, polymers	Low	Low	Yes
micro stereolithography	mm–cm	µm–cm	Photoresists, light curable monomers	Low	Medium	No
3D printing	mm–cm	100 µm–cm	Metals, polymers	Low	Medium	No
two photon polymerization	µm–mm	nm–µm	Photoresists, photoactive hydrogels	High	High	No

Table 2: Comparative overview of one-step manufacturing techniques (taken from ref. [40])

Common used materials for chips are metals, glass and silicon and mainly polymers as acrylates and vinyl polymers, epoxy resins, thiolenes, polyurethanes and siloxanes. The polymers can be physical classified by duroplastic polymers, thermoplastic polymers and elastomers [40].

The common used thermoplasts are:

Poly(methyl methacrylate) (PMMA, of methyl methacrylate) is used to realize lab-on-a-chips for electrophoresis and for the separation of DNA [44, 45]. PMMA has avery low auto fluorescence which makes the material useful for optical applications [46]. Polycarbonate (PC, by reaction of bisphenol A and phosgene) is used for manufacturing of microfluidic mixers [47]. Polyoxymethylene (POM, polymerized from formaldehyde) is a suitable material for microfluidic capillary electrophoresis [48]. Polystyrene (PS, polymer of styrene) which was used as substrate material for cell culture devices and capillary electrophoresis studies [49, 50]. Polysulfone (PSU) a material for the encapsulation of droplets in microfluidic devices [51]. Polyetheretherketone (PEEK, by step growth polymerization of difluorobenzophenone and hydroquinone salts) used for lab-on-a-chip systems for fluidic pre concentration of analyzes for mass spectroscopy [52]. Polyethylene (PE, which is the polymer of ethene) used for the creation of devices for capillary zone electrophoresis [53]. Polyvinylchloride (PVC, the polymer of vinyl chloride) a polymer for the creation of microfluidic pumps [54]. Polyethylene terephthalate (PET, which is polymerized from its monomers terephthalic acid and ethylene glycol) which has been used for the creation of microfluidic structures for capillary zone electrophoresis [53]. Cyclic olefin copolymer (COC, by copolymerization of cycloalkenes) suitable for for blood typing on a chip [55]. Polypropylene (PP, polymer of propene) a material used as substrate material for optical biosensors in CD format and used as a material for membranes on chip [56].

Material	Hydro-carbons aliphatic/ aromatic/ halogenated aliphatic	Mineral acids	Organic acids	Bases	Organic solvents	device function
Glass	+/+/+	+	+	+	+	optical clear basal support
Silicon	+/+/+	+	+	-	0+	microstructure, replication molds
Silicon dioxide	+/+/+	+	+	+	+	microstructure, replication molds
Duroplastic polymers (thermosets)						
Epoxy resins (SU-8)	+/+/0-	+	0	+	+	microstructure, replication molds
Polyurethane	0+/0+/-	0+	-	0+	-	channel creation and sealing
Thermoplastic materials (thermoplasts)						
PMMA	+/-/-	0+	-	0+	-	electrophoresis
PC	0+/0+/-	0+	0+	-	-	microfluidic mixers
POM	+/+/0-	0+	0+	+	+	capillary electrophoresis
PS	-/-/-	0+	+	+	-	basal support for cell culturing
PSU	-/-/-	+	+	+	-	droplet generator
PEEK	+/+/-	0+	0	+	+	concentration gradient
PE	+/0/0+	+	+	+	+	electrophoresis
PVC	+/-/-	+	+	+	-	microfluidic pumps
PET	0/-/0	0	-	-	-	microfluidic structures, membranes
COC	-/-/-	-	+	+	+	blood typing
PP	+/0/-	+	+	+	+	membranes
Elastomers						
PDMS	-/-/-	0+	0+	0-	-	channel creation, sealing, membranes

Table 3: Chemical compatibility commonly used materials for microfluidic devices; good compatibility (+) to medium (short time) compatibility (0) to non-compatible (-) with respect to the given solvent

Materials are treated with solvents to bond to each other to build chips out of composed designs. Beside the functional aspect the chemical compatibility has to be considered (see Table 3). Another

key factor is the influence of chosen material on the cell culture. The stiffness of material can influence differentiation of cells and their migration behavior [57].

As mentioned before the golden standard is the use of the the elastomer PDMS. The major advantages are it is inexpensive, easy to fabricate by replication of molds, flexible, optically transparent, biocompatible and its fabrication does not require high capital investment and cleanroom conditions [42]. Beside the widespread use of soft-lithography techniques PDMS can be structured through wet and dry etching, photolithographic patterning of a photosensitive PDMS and laser ablation [42].

However, PDMS absorbs small hydrophobic molecules, which could significantly affect the drug concentrations in lab-on-a-chip devices with high surface-to-volume ratio. This restricts the use of PDMS-based devices drug development application[1].

Furthermore PDMS can causes problems for in-chip cell cultivation and manipulation through the leaching of uncross linked oligomers, deformation of channels and cell chambers, as well as gas permeability, which can lead to evaporation and changes in medium composition and osmolarity[43]. On the other side it also has physical drawbacks as short-term stability after surface treatment and incompatibility with very high pressure operations [42]. Therefore there is important need on having alternatives beside PDMS [58, 59, 60].

2.4 Bonding and sealing of lab-on-a-chip systems

A membrane-integrated cell-based lab-on-a-chip system needs stacked layers of micro fabricated cell culture chambers to reconstructed micro physiological environment. The bonding steps assures that the device is representing a robust and closed microenvironment. The combination of materials bonded to each other restrict the chip design. The lab-on-a-chip needs to be sealed and bonded proper to (1) confine solvents, samples and reagents in defined volumes, (2) prevent uncontrolled spreading of liquids along wettable areas, (3) reduce contamination and biohazards, (4) minimize adversary evaporation of samples and reagents from chips, and (5) protect sensitive and fragile structures or molecules from dust or physical impacts [42]. Depending on the material which is bonded or sealed different approaches like physical, thermical or chemical can be taken in regards of the compatibility of the materials [58, 59, 60].

During a running experiment a chip can be under mechanical stress by the applied pressure. This pressure in the channels results in tensile force. The adhesive layers, the weakest part of the chips, have to handle those tensile forces.

Sealing by conformal materials as PDMS, which can be sealed to itself or other substrates both reversibly and irreversibly without an adhesive. PDMS structures can also seal other plane components, such as silicon, glass, or plastics even though having metal electrodes [42].

The design needs to replicate the cellular heterogeneity and multilayered tissue structures found in all organs and should give a advantageous for co-culture of different cell types. The key element is redesigning this physiology aspect in a lab-on-a-chip. Semipermeable membranes with pores in the scale of a few micrometers are commonly used as cell culture basal supports bonded between two perfused channels. Through this set up, the membranes is a physical barrier to cell migration while permitting their exchange of soluble signaling molecules through the pores, mimicking the role of a tissue barrier in vivo. This approach helps to study different types of tissue–tissue interfaces and immune responses, bimolecular transport, gas and fluid exchange, drug delivery, and nanoparticle absorption [61]. The big disadvantage of those commercially available or custom-designed semipermeable membranes is that the are made up of synthetic polymers, such as polyesters, polycarbonates, or PDMS, which significantly differ from the native natural cell environment [61]. PDMS for example needs special surface treatments to be bonded to membranes [62]

A membrane is defined as s a semi-permeable barrier. The membrane controls the transport of cells and medium. The crucial part is to fabricate those in a lab-on-a-chip by several methods: (1) direct incorporation of membranes, (2) membrane preparation as part of the chip fabrication process, (3) in-situ preparation of membranes and (4) use of membrane properties of bulk chip material [62].

Incorporating the membrane not proper can results in a bonding problem which leads to a leakage of the system. This occurs especially for combining glass or silicon with polymeric membranes and

PDMS for example needs special surface treatments to be bonded to membranes [62].

2.5 Pressure sensitive adhesive tapes

Pressure sensitive adhesive tapes are clear, thin flexible plastic coated film coated on both sides with a medical grade pressure-sensitive adhesive. The double-faced tape is protected by polyester release liners on both sides.

The tapes have non-migratory acrylic adhesives, tight thickness tolerance and a flexible adhesive system. The benefits of those tapes are facilitating design options, allowing lateral flow in membrane-based devices, high tack and peel properties, adhering to a variety of substrates including low energy surfaces, low outgassing, barrier to evaporation and low auto-fluorescence (Adhesives Research).

They are developed for bonding, laminating and assembly of in-vitro diagnostic and related membrane-based immunoassay products. Their defined hight determines the hight of the structure which is a design restriction.

2.6 Required material properties for lab-on-a-chip system
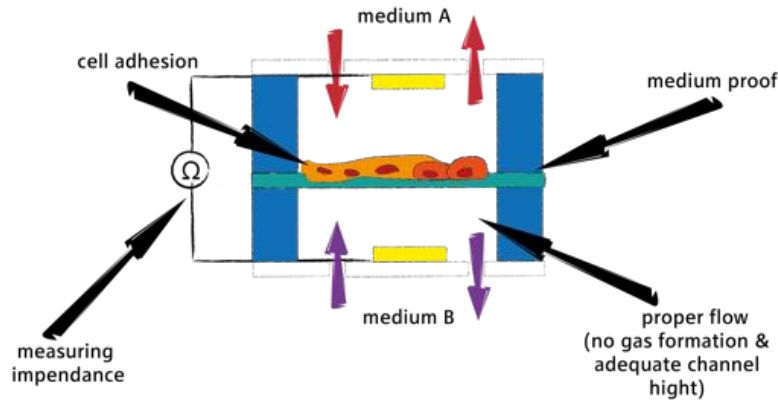

Figure 5: Requirements for membrane- and electrode-integrated cell-based lab-on-a-chip system

A lab-on-a-chip system requires proper flow as well as a medium proof structure (see Figure 5). Furthermore glass with the integrated electrodes needs to be incorporated as the basal and sealing layer. To enable a working membrane- and electrode-integrated cell-based lab-on-a-chip system different crucial aspects has to be considered. First of all all the materials have to be machined before they are bonded together to represent a vapor proof dynamic cell culturing system. The lab-on-a-chip system should have a maximum of vapor impermeability to avoid cross contamination of the cells seeded in the chip and maintain a stable microenvironment [42]. With PDMS as a gas permeable material there is still a need of sealing materials to control gas exchange as a parameter in the chip. As mentioned before the placenta barrier regulates the nutrient and gas exchange for the fetus [8]. To investigate this role a gas proof system is necessary to mimic precisely this microenvironment and distinguish the gas concentration. This would establish a membrane model where the essential key function, oxygen and glucose transport, can be controlled and measured. A gas proof system helps to model an under-supply of oxygen (hypoxia) which significantly influences the behavior of the tissue of the placenta [63]. A high hydrophilicity leads to proper perfusion of the system as well as avoids bubble formation which causes stress to cells cultured in the chip. The other key aspect is the biocompatibility of the materials and the importance that they have minimal influence on the cell viability. Cell compatibility is quantified by either Life and Dead staining of the cells [14] an the viability compared between the

19

exposure and absence of the material [15]. For fluorescence staining assays and optical analytics no influence of the absorption spectrum and the emission spectrum is required.

2.7 World-to-chip interface

The set up of the world-to-chip interface have great impact on the manufacturing cost and performances of the final devices[42]. Actual technics allow to manufacture lab-on-a-chips systems with in the scale of micrometers. This results in working within the range of microliter. Therefore fluidics has to be maintained and controlled precisely by the use of integrated or external pumps and valves. Beside the interconnection of flow, sensitive data has to be gained to maintain, observe and analyze the microenvironment. The observation and analysis are carried out by optical-, electrical- or magnetic-based techniques (see Figure 6).

This results in the challenge to connect the lab-on-a-chips system to its complex experimental set up on the one hand and that it is still user-optimized on the other hand. The experimental set up heavily influences robustness and performance of the system. The maintaining of lab-on-a-chips via a interface has been neglected in the past but through the rising importance for research application the market with world-to-chip solutions is increasing [1].
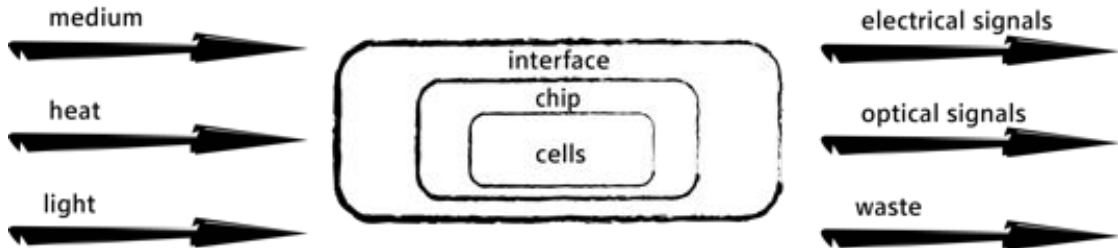

Figure 6: Interface as an input/output System with fluidic, temperature regulation and light as inputs and electrical and optical signals, and waste as an out put

Because of the vast variety of different microfluidic devices a broad spectrum of designs are given. The designs differ significant in scale, materials and fabrications technics and also incorporate many different functional elements. With the aim to go down in size but increasing the complexity of the systems often many several prototypes and design iteration are carried out. There is a need for reliable, low-cost and convenient interfaces to connect the chip to the outside world and having a suitable set up for efficient device operation.

The input/output complexity of lab-on-a-chip system increases with complexity of the model, to be more precise the model of the organ. Membrane- and electrode-integrated cell-based lab-on-a-chip systems need a proper support of fluid interconnections to all the channels as well as electrical interconnections for the TEER readout. The special experimental set up needs manual handling and plugging by the operator, which induces additional constraints on the final interface due to practical reasons.

As interconnection between the chip and the interface, lab on a chip systems can (1) be sealed with a cover layer with manual drilled or punched holes as inlets and outlets for fluidic/electrical interfaces, (2) chemically-treated for tuning the wetting properties of surfaces and modulating protein-surface interactions, (3) indented or fully diced to produce individual chips, and (4) connected to peripheral devices such as pumps and valves using inlet/outlet ports. In this study a set up by connecting the lab-on-a-chip system via inlet/outlet ports to peripheral devices such as pumps and valves is considered to resort to the existing lab infrastructure.

Aside from bonding and fabricating devices, the function of the lab-on-a-chip system is depending on a reliable fluidic interface between the chip and the experimental set up (e.g. external pumps,

valves, tubings, etc). The fluidic interfaces are known as "fluidic interconnect", "world-to-chip" or "macro-to-micro" interfaces[42].

The chip can be connected through interbased connections as gauge needles into PDMS, male and female PDMS connectors or integrated custom-made PDMS rings with metal tubes [64]. Insertion-based reversible interconnects as compression based interface with soft intermediated elements as O-rings, PDMS or silicone tubings can handle higher pressures [42].

The fluidic interface should hit the following needs: (1) minimal dead volume, (2) avoid cross-contamination of samples, (3) be easy to plug, (4) be removable and reusable, (5) be reliable at high pressures, (6) be small enough to allow high density connections, (7) be made using simple and low-cost techniques, (8) be chemically inert, and (9) be compatible with commercial tubings and fittings [42].

The big variety of existing lab-on-a-chip interfaces with all the features can be sorted by the plugging orientation (i.e. in-plane or out-of-plane), material of the microfluidic device (e.g. PDMS, plastic, glass/silicon, etc), pressure capability, and maximum number of connections that can be achieved simultaneously. On the other side the common connection technics are: (1) reversible insertion of micro-needles or tubes into holes drilled or etched on the chip surface or edge, (2) reversible fluidic connection with direct contact to the surface of the device by compression sealing, (3) application of an adhesive to achieve a high strength and permanent interface, and (4) monolithic integration of microfluidic ports [42].

Unfortunately there is no wide spread standard of electrical connection for lab-on-a-chip. Card edge connectors and spring-loaded contacts, as well as some of the advanced packaging techniques developed for integration of active sensors are recently emerged technologies for electrical connections [42].

2.8   Aim of this study

The aim of the study is to establish a working membrane- and electrode-integrated cell-based lab-on-a-chip system in a running interface. First of all the needs for engineering a reliable membrane- and electrode-integrated cell-based lab-on-a-chip system are identified. The key factor driving the engineering efforts is rapid and user-friendly prototyping for a short concept-to-chip time. This is needed for working under the experimental set up with perfusion and incubation. For that reason biocompatible pressure sensitive double-sided adhesive tapes are chosen. After defining each engineering step those pressure tapes are evaluated against each others and PDMS, the most common material used for microfluidic and lab-on-a-chip.

For evaluating the machining and further manufacturing of chips out of the different materials, the manufacturing processes are analyzed in regards of dimensional tolerances within the microstructures. To support bigger structures within the chip, powder blasting is as well analyzed as a way to manufacture chip sealing and channel structures out of glass. After establishing a proper way to build up single channel based and multiple channel membrane based chips, an interface is developed. The interface is tested to maintain the experimental set-up for the membrane- and electrode-integrated cell-based lab-on-a-chip system. By having a working way to manufacture chips with membranes and maintain those, the pressure sensitive double-sided adhesive tapes are further tested to quantify there impermeability to medium vapor (for having a closed fluid system during the experiment) and the ability to bond to glass and membranes by testing the tensile and shear strength of those bondings (to fulfill the important issue to have a robust membrane based chip). To create a cell based lab-on-a-chip system the the surface properties of pressure sensitive double-sided adhesive tapes are measured in regards of hydrophilicity. Furthermore the viability as well as dying of cells in an over exposure of the adhesive substance is evaluated. In case of further optical assessments of the chips, the absorption spectrum of the pressure sensitive double-sided adhesive tapes are measured. For the most common fluorescence methods the emission spectrums are measured.

Different membranes are tested by the way cells can adhere to them and the pressure sensitive double-sided adhesive tapes can bond to them. Based on those insights the adequate membrane for the membrane based set up is chosen.

After the quantifications a membrane- and electrode-integrated cell-based lab-on-a-chip system is build out of the best materials for the best combination out of the adhesive tapes, glass and membranes. The chip is put into the experimental set up with placenta cells with in the designed interface. To have a proper and sensitive tool to model the human placenta barrier and observe it, the chip needs to stay stable for 7 days in regards of designed structure, medium tightness and the maintaining. The tool will be useful in understanding how drugs and nano particles can pass and destroy the placenta barrier. Further more this tool can be used to model other membrane interfaces in organs. In the end a TEER measurement is conducted over 7 days to have a proof of principle for the working membrane- and electrode-integrated cell-based lab-on-a-chip system.

3 Materials & methods

3.1 Pressure sensitive double-sided adhesive tapes

ARcare 92712Ⓡ (Adhesive Research) is a clear pressure sensitive double-sided adhesive tape out of a 12.7 µm thick polyester film with MA-93 as an acrylic pressure sensitive adhesive (17.78 µm on each side) with results in a total thickness of 48.26 µm (with liners 149.86 µm).

ARcare 90445Ⓡ (Adhesive Research) is a clear pressure sensitive double-sided adhesive tape out of a 25.4 µm thick polyester film with AS-110 acrylic medical grade adhesive (27.94 µm on each side) with results in a total thickness of 81.28 µm (with liners 182.88 µm).

ARcare 90106Ⓡ (Adhesive Research) is a clear pressure sensitive double-sided adhesive tape out of a 25.4 µm thick polyester film with MA-69 acrylic hybrid medical grade adhesive (58.42 µm on each side) with results in a total thickness of 142.24 µm (with liners 243.84 µm).

ARsealⓇ (Adhesive Research) is a clear pressure sensitive double-sided adhesive tape out of a 50.8 µm thick polypropylene film with SR-26 silicone adhesive (45.72 µm on each side) with results in a total thickness of 142.24 µm (with liners 243.84 µm).

3.2 Micro machining of glass using powder blasting

Glass was machined using powder blasting with a Sandstrahlkabine SMART Cab (Logiblast Austria) and Edelkorund F120 (Logiblast Austria) at 3 bar. Except as noted otherwise Sandblast Super foil (500 µm) (Gemba Ges.m.b.H Austria) was taken as mask for powder blasting. The mask was designed by AutoCAD 2017 (Autodesk) and than copied into CutStudio (Roland). Cutting was performed by a CAMM-1 Servo GX-25 (Roland) with a ZEC-U1715 (Roland) blade. The pictures of the blasting quality were analyzed by using FIJI software. For identify a mask foil with convenient properties ASLAN S62 (600 µm), ASLAN S64 (330 µm), ASLAN S66 (230 µm), ASLAN S68 (180 µm) and ASLAN S69 (80 µm) was taken as well (all by IFOHA GmbH + Co.KG Germany).

3.3 Micro machining of pressure sensitive adhesive using plotting

All needed shapes out of the pressure sensitive double-sided adhesive tapes where machined as followed: first the needed design was created with AutoCAD 2017 (Autodesk) and than copied into CutStudio (Roland). Cutting was performed by a CAMM-1 Servo GX-25 (Roland) with a ZEC-U5032 (Roland) blade (see section A.3 and A.7). The pictures of the cutting quality were analyzed by using FIJI software. Except as noted otherwise the following setting were used for each tape:

material	blade extension	cutting force [gf]	cutting speed [cm/s]	blade off set [mm]	cutting quality
ARcare 92712	220 µm	80	20	0.25	HEAVY
ARcare 90445	220 µm	80	20	0.25	HEAVY
ARcare 90106	220 µm	100	20	0.25	HEAVY
ARseal 90880	220 µm	100	20	0.25	HEAVY

Table 4: Cutting settings for pressure sensitive double-sided adhesive tapes

3.4 Membranes

For identifying the best membrane for cell culturing within the membrane- and electrode-integrated cell-based lab-on-a-chip system different membranes with in chips has been taken into account: WhatmanⓇ CycloporeⓇ polycarbonate membranes (Sigma-Aldrich), WhatmanⓇ Nuclepore™ Track-Etched

polycarbonate membranes PVP-free pore size 5 µm (Sigma-Aldrich) and ipCELLCULTURE™ track etched polyester membrane (pore size 3 µm, pore density $8 \cdot 10^5 cm^{-2}$, thickness 9µm).

3.5 Assembly of multi layered lab-on-a-chip devices

The glass slides were sputtered with Cr/Au/Ag, patterned using liftoff lithography, were first powder blasted to create the holes for connecting the channels to the interface (see Figure 26 A), afterwards washed with water, and the silver surface was chlorinated with 50mM FeCl$_3$ for 40s and cleaned with distilled water. The glass slides for the channel structure or connecting holes were powder blasted and washed (see section A.2). As adhesive material ARcare 90445 was used in the according dimension (see Figure 26 B) and ARcare 90106 as a sealing material between the chip and the interface. Holes through the membrane were punched with a biopsy puncher (1.5 mm).

The PDMS design was created with AutoCAD 2017 (Autodesk) and than copied into CutStudio (Roland). Cutting was performed by a CAMM-1 Servo GX-25 (Roland) with a ZEC-U5032 (Roland) blade. The PDMS to glass bonding was performed by plasma activation (high) for 1min and curing between clamps overnight at 70 ⁰C. T

All parts bonded to the pressure sensitive adhesive tapes were aligned by hand and bonded together by applying pressure manual.

3.6 3D printing

Parts for 3D printing were designed with FreeCAD Software and printed with a Original Prusa i3 MK2S printer (for printer settings see sectionA.1) with a layer hight of 0.2 mm, perimeters of 3, top and bottom solid layer of 2 and a rectilinear fill pattern with 10% density. The printing speed was: perimeters 60 mm/s, infill 80 mm/s and travel 130 mm/s. The PLA filament has a diameter of 1.75 mm and is extruded with 220 ⁰C and printed on the bed with 55 ⁰C.

3.7 Cell culture

BeWo b30 cells (EMPA, Switzerland) were cultured in Dulbecco's Modified Eagle's Medium (DMEM with L-glutamine and high glucose; Gibco, 11965-084) with Ham's Nutrient Mixture F12 and 10% Fetal Calf Serum (FCS, PAA, A15-101) and 1% Antibiotics (Gibco, 15240-062) at 37⁰ C with 5% CO_2. When cells were cultured with in a chip 1% HEPES, STERILE, 1M, pH 7.3 (AMRESCO LLC) was added to the culture medium. For the measurement TEER the first day medium was exchanged manual and at the second day the chip was perfused with 2 µl/min by a OEM 310 – Full-size neMESYS OEM Pump (CETONI). For opening out the cell monolayer Trypsin was used after washing with Phosphate Buffered Saline in total three times.

To determine the needed amount cells per cm^{2}to have a proper confluent monolayer after seeding different amounts of cells were seeded into a 48 well plate and pictures have been taken 1 day, 2 days and 3 days after seeding. Following amounts has been seeded (density [cells/cm^2] / cells per well): 12.5k / 11.9 k, 25k / 23.8k, 50k / 47.5k, 100k / 95 k, 200k / 190k.

For cell culturing membranes has been washed with ethanol for 30min then flushed two time with Phosphate Buffered Saline (PBS) and one time flushed with cell culture medium. If mentioned the membranes were treated with Collagen Type I from rat tail (Sigma-Aldrich) for 30min and afterwards flushed with culture medium. Cells were seeded with 100k cells/cm^2.

3.8 Design & manufacturing of the world-to-chip interface

The chip fixture as well as the connectors for tubes, electrodes were designed with FreeCAD Software and printed with a Original Prusa i3 MK2S printer. To connect the interface with the chip tubes FEP Nat 1/16x.030x100ft - (1520XL Upchurch Scientific) with P-200X - Flangeless Ferrule Tefzel™

(ETFE), 1/4-28 Flat-Bottom, for 1/16 (IDEX Health & Science LLC) were used. For screwing M3 screws and nuts from stainless steel were used.

To evaluate the pressure sensitive Double-Sided Adhesive Tapes with the best sealing properties between interface and chip, a sample of each tape was glued on top of a glass slide. The glass slide with the tape was mounted in the interface and tightened carefully so that the tube connectors are placed directly on the tape. For every new material a new set of flangeless ferrules were used to avoid residual adhesive material from former experiments. The interface was tightened manual. The whole interface including the chip was placed in a water bath to show bubble formation in case of leakage. To test the degree of sealing of each tape was tested by applying air pressure increased stepwise with 1 bar every 30 seconds with in the ports until bubble formation was seen. To further determine the degree of sealing of ARcare 90106 the same set up as above was conducted with applying 5 bar for 8h.

3.9   Longterm leakage testing

To proof the longterm functionality of the interface with ARcare 90106 as sealing material two chambers in series of a chip (see Figure 14 A) were perfused with dyed water (to enhance visibility) with 2 µl/min for 4 weeks (in total 4 ports). The experiment was checked every two days for leakage.

3.10   Medium vapor transfer rate

The chips were filled with cell culture medium and sealed with Adhesive qPCR Seal (Sarstedt). The initial weight of each chip was measured. Afterwards all chips were placed on a heating plate at 36.5 ºC for 24h. The weight was measured after 2h, 4h, 8h and 24h and subtracted by the initial weight to calculate the mass loss through evaporation. This weight loss was divided by the area of the channel wall of the pressure sensitive double-sided adhesive tape or PDMS with the assumption that either the glass, the membranes and the qPCR tape is total proof to the medium. The mass loss per area was calculated in $\frac{mg}{mm^2}$. The medium medium vapor transfer rate is given in $\frac{mg}{mm^2 h}$.

3.11   Contact angle of water

To identify the hydrophilicity of each adhesive surface and compared it with PDMS and glass, a sample of each tape was bonded manual on top of a glass slide. The PDMS sample was placed on a glass slide as well. A drop of 10 µl of distilled water was placed on top of the sample and picture taken. The angle of each drop was determined with Adobe Illustrator (Adobe Systems).

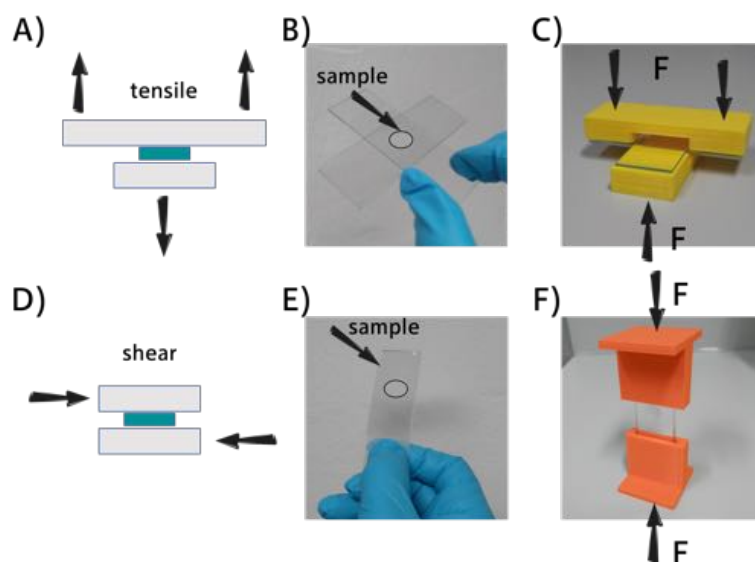## 3.12 Tensile and shear strength test

Figure 7: A) schematic sketch of applied tensile force (sample turquoise, glass grey) B) sample for determine tensile strength C) sample within fixture for measuring tensile force D) schema off applied shear force (sample turquoise, glass grey) B) sample for determine shear strength C) sample within fixture for measuring shear force

For sample preparation glass slides have been washed according to section A.2. For determining the tensile and shear strength (see Figure 7 A and D) of each tape in regards to bonding to glass a circular sample with an area of $1cm^2$ was bonded between two glass slides (see Figure 7 B and E) with 250 N applied for 1 min in a shop press WP 20H (HOLZMANN MASCHINEN GmbH) with a precision tension and compression load cell 8524 (burster GmbH & co kg). For testing the strength of bonding to membranes the same procedure as before was conducted by placing a membrane between two samples between the glass slides. Force was applied by a rate of approximately 10 N/s. The membrane including samples have been checked after each rupture that the sample detached from the membrane and not from the glass. The numbers in brackets indicate the number of samples where the glass has been broken before the sample detached (see Figure 17).

3.13 Bio compatibility and viability assay

To evaluate the the cell compatibility with the adhesive layer a sample (circular with 13 mm diameter) of each tape was bonded on the bottom of a well in 24 well plate. Afterwards 190 k cells (100k per cm^2) were seeded on top. Pictures were taken 24h and 48h after seeding. For life/dead staining Calcein AM (Thermo Fisher Scientific, 2µl per ml culture medium) and Ethidium Homodimer-1 (Thermo Fisher Scientific, 4 µl per ml culture medium) was used. Pictures of life/dead staining has been taken after 30 min of incubation with Calcein AM and Ethidium Homodimer-1. The life/dead staining was conducted with samples after 24 h and different samples after 48 h (see section B.6). To quantify cell viability Prestoblue (Thermo Fisher Scientific, 10% of the total medium in culture, incubated for 30 min) was used after 24 h and after 48 h in different samples (see section B.7). For quantification a EnSpire 2300 plate reader (PerkinElmer) was used and culture medium with Prestoblue was taken as an off set value. Samples with out any material has been taken as reference for a viability of 100%.

3.14 Evaluation of optical properties

Glass slides has been washed and samples has been bonded between two glass slides with 2500 N for 1 min. The sample of PDMS was prepared as mentioned in section 3.1. For quantification of the absorption spectrum (300-700 nm) a EnSpire 2300 plate reader (PerkinElmer) was used and two plain glass slides has been taken as a base line value (see section A.9).

The same samples as mentioned in the section Absorption above has been taken to determine the emission of the materials. For quantification of absorption a EnSpire 2300 plate reader (PerkinElmer) was used and two plain glass slides has been taken as a base line value (see section A.10). The excitations and corresponding emission spectrum was measured for: 358 nm / 378-700nm, 488 nm / 508-700nm and 553 nm / 573-700 nm.

3.15 On chip TEER measurement

For cell culturing the chip has been washed with ethanol for 30min then flushed two time with Phosphate Buffered Saline (PBS) and one time flushed with cell culture medium. Then the chips was treated with Collagen Type I from rat tail (Sigma-Aldrich) for 30min and afterwards flushed with culture medium. Cells were seeded with 100k cells/cm^2.

TEER was measured with a EVOM2 Epithelial Volt/Ohm (TEER) Meter (World Precision Instruments). The EVOM2 was connected through crocodile clip to desoldering braid which were soldered to the electrodes of the chip. All TEER measurements has been taken after at least a heating up phase of 20min of the EVOM2. The big electrode was connected as I1 (corresponding I2) and the small electrode as V1 (V2).

4 Results & discussion

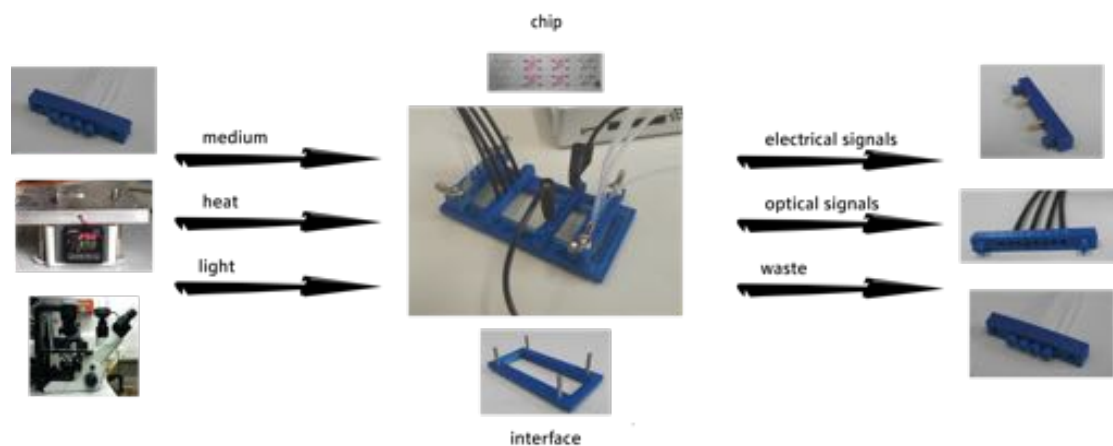## 4.1 Optimization of world-to-chip interface

Figure 8: Standardized interface with inputs and outputs for lab-on-a-chip systems on standard microscope glass slides

A fluidic world-to-chip interface should hit the following needs: (1) minimal dead volume, (2) avoid cross-contamination of samples, (3) be easy to plug, (4) be removable and reusable, (5) be reliable at high pressures, (6) be small enough to allow high density connections, (7) be made using simple and low-cost techniques, (8) be chemically inert, and (9) be compatible with commercial tubings and fittings [42]. A standard microscope slide is chosen as base for the interface design. They are found in plenty lab-on-a-chip application as well in biology, tissue engineering and chemistry. The microscope slides based interface is designed to support the chip with cell culture medium as a fluid as well as the read out of the impedance for the TEER interface (see Figure 8).
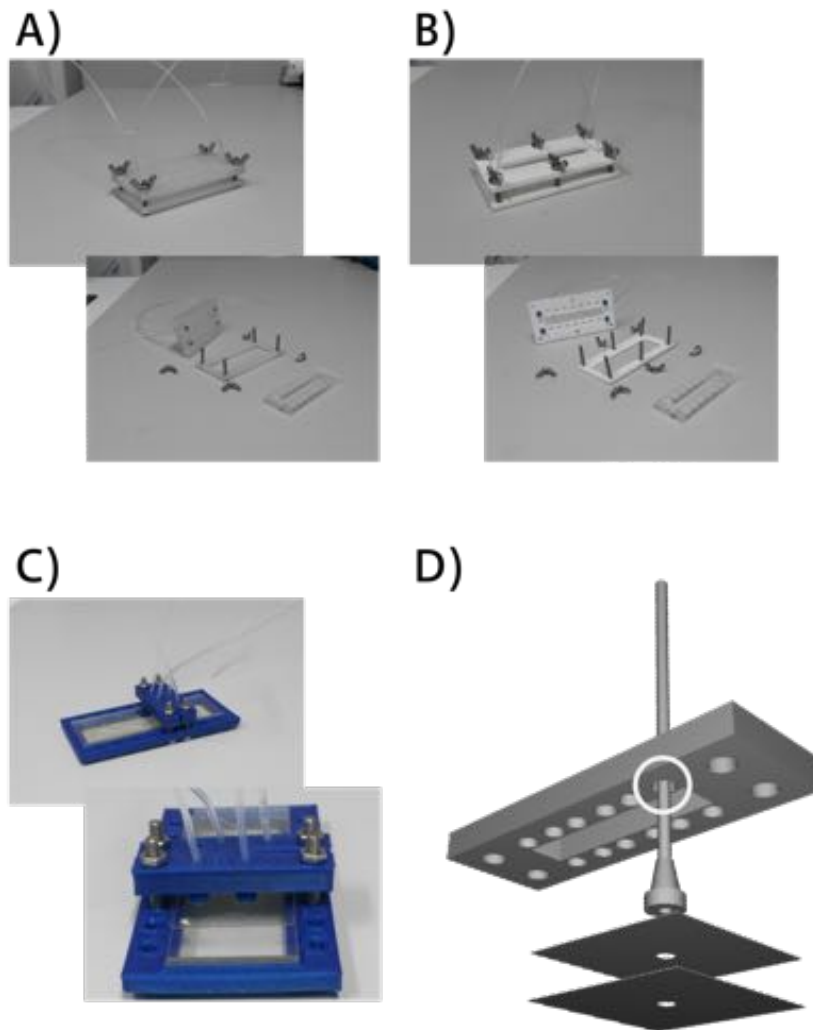
Figure 9: Different prototypes of interfaces for fluidic connection with commercial available tubes FEP - 1520 tubes (Upchurch Scientific) and P-200X - Flangeless Ferrule (ETFE) A) first prototype with four point fixation of the two parted tube connector and the casted PDMS sealing for between chip and interface. B) second prototype with six point fixation of the single parted tube connector and the castet PDMS sealing for between chip and interface. C) final model with two point fixation for each fluid interconnecting row and pressure sensitive double-sided adhesive tape as a sealing material D) schematic illustration of interconnection of the chip (lower plane), pressure sensetiv double-sided adhesive tape (upper plane) the flangless ferrule and the conical shaped (white circle) fitting within the upper frame.

After some iteration steps (see Figure 9 A and B) the design was shifted from using a thick layer of PDMS as an elastic sealing to the use of a pressure sensitive double-sided adhesive tape (see Figure 9 C) . This step was necessary to increases the density of possible fluid connections per chip up to 24 ports and to decreases the time for reproducing a complete set of all parts for a interface. Here it is taken into account that reprinting all parts for one interface and ensemble those won't take longer than 2h. With this design it is possible to have minimal dead volume by directly connecting the tube ending on the chip (see Figure 9 D). By having single inlets and outlets cross-contamination is avoided. The

29

use of a screwable and easy to assemble interface makes it easy to mount chips. Beside the advantage of using commercial available parts which are compatible with different systems, it is assured that the parts in touch with the fluidics and the cells are chemically inert and biocompatible as well as autoclave-able.

This design has fluidic connection based on a gasket out of pressure sensitive double-sided adhesive tape which seals under pressure. Conical connection between the tubings and the flangeless ferrule tighten itself by being screwed of the interface. Here must be highlighted that the most crucial part is this tightening process. While mounting glass chip, the chip can break very easily by applying to much pressure by the interface. How ever the interface can be tightened softly in the beginning and in case of a still leaking chip tightened afterwards.

To evaluated the sealing quality of pressure sensitive adhesive tapes in the intermedia surface between the chip interface the handled peak air pressure was measured.
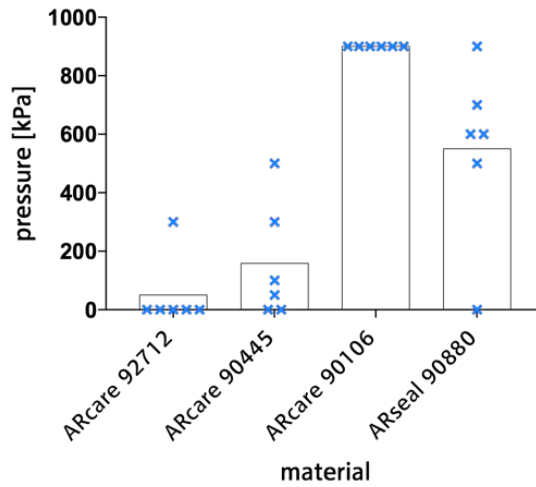

Figure 10: Peak air pressure test of different pressure sensitive double-sided adhesive tape with the mean of each measured value (blue crosses) (p_{max}=9 bar)

As illustrated in Figure 10 ARcare 90106 shows the best ability to seal the glass/flangeless ferrule interface under air pressure. Compared to the other tapes ARcare 90106 has with MA-69 acrylic hybrid medical grade adhesive (58.42 µm on each side) the thickest adhesive layer (see section 3.1). ARcare 90445 is manufactured with the same 25.4 µm thick polyester film but shows poor sealing quality. The MA-69 acrylic hybrid medical grade adhesive compared to AS-110 acrylic medical grade adhesive provides with better sealing properties. ARcare 92712 shows the poorest sealing properties. The variation within the measured peak air pressure is caused by dust and small particles of the lab environment which pollute the adhesive surface. ARcare 90106 and ARseal 90880 have better sealing properties between up to 900 kPa, where ARcare 92712 and ARcare 90445 provides only sealing up to 500 kPa. Those trials were carried out by manual tightening which represents the ordinary lab procedure.

Compared to interbased connections as gauge needles into PDMS (which handle a pressure up to100kPa up to 700 kPa) [65], ARcare 90106 provides sealing at least up to 900 kPa. This is a suitable high value compared to fabricated male and female connectors using replica molding of PDMS and tested the connectors at pressures up to 103 kPa [66] or the integrated custom-made PDMS rings in PMMA microfluidic chips which can handle 750 kPa pressure by metal tubings [67].

The insertion-based reversible interconnects are suit able for quick and easy mounting of chips because they do not require fixtures or frames for applying a significant compression force to ensure

leak-free connections. By using a compression based interface with soft intermediated elements as O-rings, PDMS or silicone tubings higher pressures can be handle [42].

PDMS can be used in a compression based interface up to 220kPa [68] but it is noted that this value can be heavily depending on the reversible connection technics used (30kPa to 1500 kPa) [64]. Magnetic connectors can handle 250 kPa (O-ring) to 500 kPa (polyamide tape) [69]. Compared to those values ARcare 90106 with in the interface is rated as proper sealing material. This design can by far not withstand the pressures applied with permanent fluidic connections and monolithic integration of fluidic connections but for membrane- and electrode-integrated cell-based lab-on-a-chip systems the range of up to 900 kPa is more than acceptable. Compared to the manufacturing of permanent fluidic connections and monolithic integration of fluidic connections the here shown design is easy and fast to produce and therefore highly adaptable.

Fluidic connections using the contact of a gasket under compression are easy-to-use, reversible and allow for multiple connections. One drawback of those connection is that they are often not able to maintain high pressures. If a adhesive connection is used problems with clogging tubings and microfluidic channels arise. Depending on the adhesive used, the time for the application and the curing can be long. The limited compatibility of some adhesives with chemicals and solvents can be cause disadvantages as well [42]. This problems are avoided by the use of the biocompatible pressure sensitive double-sided tapes which can easy cut in the scale of several hundred microns for the gasket. The tapes are pressure sensitive, there is no time needed for application and the curing of the adhesive. The tape as gasket adhere to the chip and has no influence on the reusability of the whole interface.

Longterm leakage test was performed since as the material with the highest adhesive properties ARcare 90106 was identified, air pressure as well as liquid leakage tests were performed for extended period of 8h at for 4 weeks respectively.

For the peek pressure test 500 kPa were applied for 8 h without any bubble formation. This states that ARcare 90106 withstands high pressures over longer periods of time even in a liquid surrounding . Next a long term fluid experiment was carried out with water and a flow rate of 2 µl/min for 4 weeks. After 4 weeks no leaking was observable and therefore the designed interface can be used for several weeks and high pressure applications.

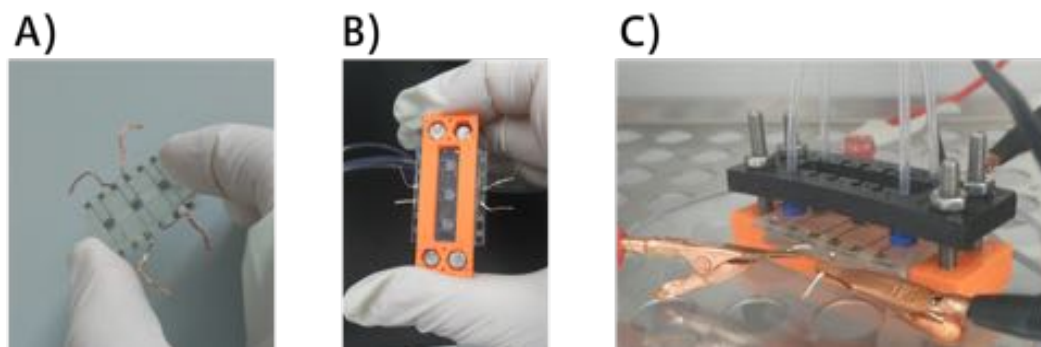### 4.1.1 Adaption of the world-to-chip interface for TEER measurement

Figure 11: Adaption of the interface for the membrane- and electrode-integrated cell-based lab-on-a-chip systems

As having the the interface design as a proven concept, the design was adapted for the membrane- and electrode-integrated cell-based lab-on-a-chip systems as showed in Figure 11. Experiments were conducted over 7 d with cells in culture. In regards of the design for the electrodes, there was no quick and easy electrode connection design established. The electrodes were connected through crocodile clip to desoldering braid which were soldered to the electrodes of the chip.

4.2 Optimization of the rapid prototyping as well as physical and biological characterization of materials

To analyze the cutting behavior of pressure sensitive adhesive tapes a defined structure was cut, residual material removed and the deformation of the edges of the structure was measured.

When the digital model for the given chip design already exist, the chip structures can be cut with in minutes. By primary evaluation of the plotting resolution structures down to 100 μm are cut. The limiting factor for the machining of the pressure sensitive double-sided adhesive tapes is how easy and under which deformation the residual material of the designed structure can be peeled of. This represents the limit of the scale for cutting structures within pressure sensitive double side adhesive tape.
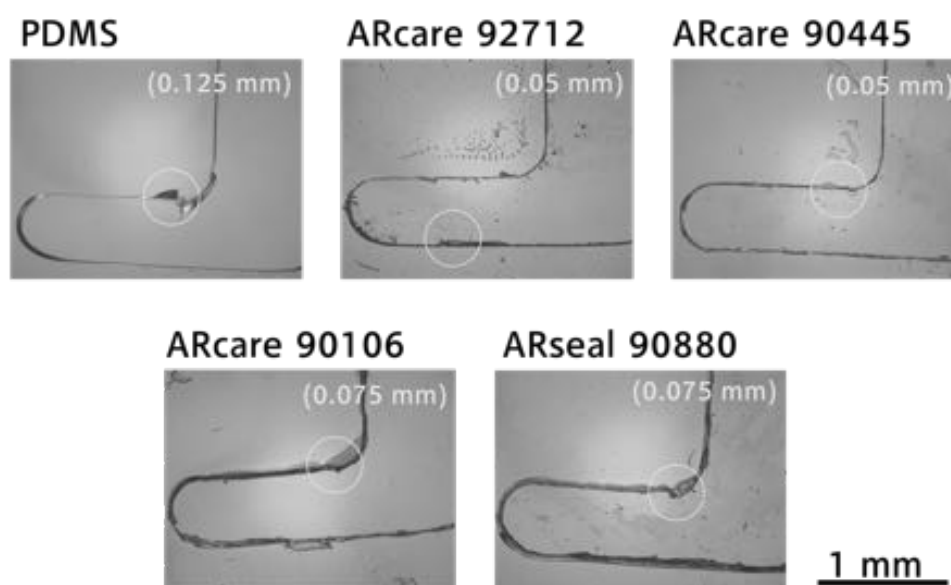

Figure 12: Cutting behavior of PDMS (250 μm thick), ARcare 92712, ARcare 90445, ARcare 90106 and ARseal 90880. The circles are marking the region with the most deformation of the designed structures. The number in brackets indicate the scale of the deformation.

Basically the proper machine set up of the cutting plotter is the base for a good machining of the pressure sensitive double-sided adhesive tapes. First of all the quality of the used blade can heavily influence the results, a new blade can produce structures down to 200 μm which can be pealed of easily, in contrast a blunt blade can't even cut the material with the same settings. Second the blade adjustment (see section A.7) determines the peel-off behavior as well. The blade should cut through the whole upper release liner film and the adhesive tape and only partly through the lower release liner. Several cutting forces were tried (from 60 gf up to 180 gf) but when the cutting force is to low the material is not cut proper and when the cutting force is to high the lower release liner is cut totally and the whole sample of the adhesive tape gets deformed in the cutting plotter. Therefore a cutting force of 80 gf was determined for ARcare 92712 and ARcare 90445 and 100 gf for ARcare 90106 and ARseal 90880. As seen in Figure 12 the adhesive tapes cut with the same blade and the settings mentioned in section 3.1 differ in the accuracy of the edges. The PDMS sample was cut with a different blade. The grey circles indicate the area with the highest deformation. For ARcare 90445, ARcare 90106 and ARseal 90880 as well as for the PDMS the deformation occurs within the inner circular border. This part is cut in the patter of a polygon to created a round structure therefore

32

many singles separated cuts are performed. This segmented cutting results in a bigger deformation compared to a structure cut in one step. The numbers in bracket indicate the scale of the deformation. When the cut structure is peeled of the adhesive layer significantly influences how precise the residual material can be removed. Therefore with the increasing adhesive layer thickness (ARcare 92712 with 17.78 µm, ARcare 90445 with 27.94 µm, ARcare 90106 with 58.42 µm, ARcare 90880 with 45.72 µm) the deformation of the structure is increasing. Beside the thickness the composition of the adhesive layer is influences the peel off behavior. Cut structures out of ARcare 90106 with a thicker adhesive layer composed of MA-69 acrylic hybrid medical grade adhesive can be removed much more easily than ARseal 90880 with a thinner layer of SR-26 silicone adhesive. Those deformation can reach up to 75 µm but only when the structure is cut with plenty several cuts. When straight structures are cut it is possible to produce channels down to a size of 250 µm with a deformation of 10%.

The vast spectrum of different manufacturing techniques for microfluidic systems range from nm with Two photon polymerization, where single molecules can be linked by a light impulse up to several 100 µm with Fused deposition modeling, where melting polymer wire in strings layer by layer applied onto each other [40]. The widespread use of PDMS to create microstructures ranges from 20 µm through creating molds by photolithography [11] up to 200 µm by cutting PDMS foil[40]. Overall the pressure sensitive double-sided adhesive tapes can be cut in the same scale as a comparable PDMS foil but with the drawback of rougher edges and a more easily deformation of the designed structure. In regards of rapid prototyping the period from concept to chip is crucial to conduct the iterative optimization steps of the prototype as fast and easy as possible, compared to the accuracy of the structure. Therefore the plotting technique of pressure sensitive adhesives is a very appropriate method because it is very fast one-step manufacturing compared to the golden standard of manufacturing PDMS.

To evaluated the machining of glass different protection foils for powder blasting are tested and the accuracy is measured.

Through cutting and removing structures in a protection foil which is deposited on a glass slide, structures can be powder blasted. Aluminum oxide particles are blasted by air pressure on the exposed glass surfaces and removing the glass. As illustrated in Figure 13 A) the pressure has to remove the glass on the one hand but on the other hand the protection foil should with stand the powder blasting until the desired structure is formed. In Figure13 A) 1 bar, 3 bar and 6 bar (from left to right) were applied. The pressure of 1 bar destroys the protection foil fewest compared to the total destroying of the protection foil with 6 bar. The pressure of 3 bars is suitable to remove enough glass and destroying the mask moderately. To evaluated which foil suits best for producing channels and holes into the glass a test template was used according to Figure 13 B). All foils tested (ASLAN S62 (600 µm), ASLAN S64 (330 µm), ASLAN S66 (230 µm), ASLAN S68 (180 µm) and ASLAN S69 (80 µm)) from IFOHA GmbH + Co.KG Germany didn't withstand the blasting through 1.1 mm thick glass (common thickness of microscope slides) as Figure 13 C) shows. The foil was destroyed before the structure was blasted in the glass. In comparison the foil of Gemba Ges.m.b.H Austria supports structures down to 1 mm in glass (see Figure 13 D). Holes with the diameter of 1.25 mm or 1.5 mm can be manufactured with a loss of 0.40 mm and holes in the size of 1.75 mm and 2.00 mm with a loss about 0.35 mm. Channels can be manufactured with a loss up to 0.7 mm of the structure. Decreasing losses are observed for increasing structure size, therefor it is easier to powder blast bigger structures compared to small structures. To further reduce the loss of the structure the glass can be powder blasted from both sides which results in a deformation of 0.25 mm (see Figure 13 E).Compared to etching which can produce precise structure in the scale of microns [40], powder blasting is only able to form structures with in the scale of millimeters. The big advantage of powder blasting is that there is no further chemical infrastructure needed to handle the high reactive chemicals for the etching process. Furthermore the glass components for the chip can be designed by the same process as the pressure sensitive double-sided adhesives. Which also results in a short concept-to-chip time.
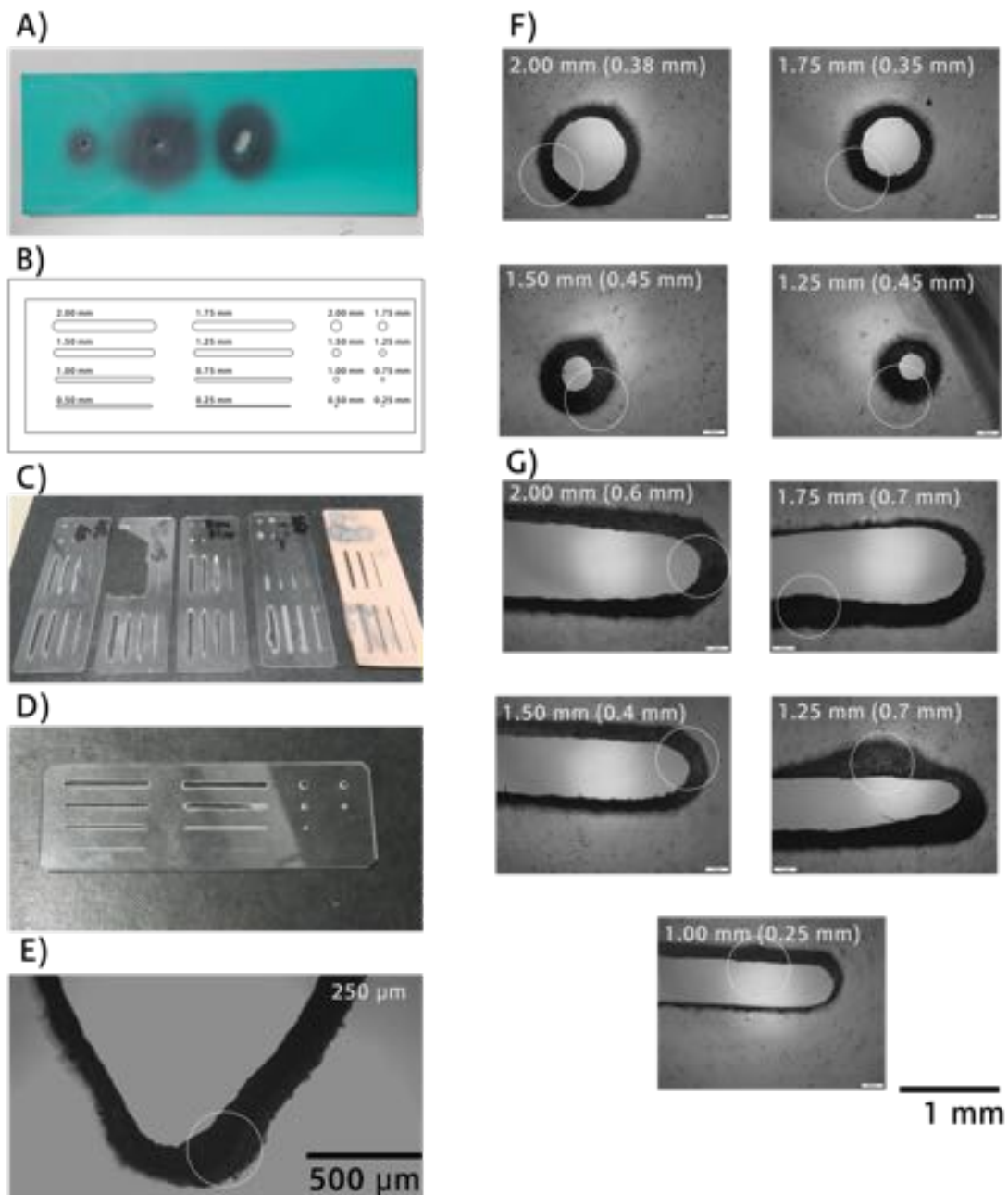
Figure 13: A) Protection foil abrasion under 1 bar (left) 3 bar (middle) and 6 bar (right); B) test mask for evaluating the blasting of straight channels (0.25 mm up to 2 mm) and holes (0.25 mm up to 2 mm); C) Test mask samples blasted with foils from IFOHA GmbH + Co.KG Germany D) Test mask blasted with foil of Gemba Ges.m.b.H Austria: E) Structure blasted from both sides, F) holes of the Test mask blasted with foil of Gemba Ges.m.b.H Austria; G) channels of the Test mask blasted with foil of Gemba Ges.m.b.H Austria; The circles are marking the region with the most deformation of the designed structures. The number in brackets indicate the scale of the deformation.

34
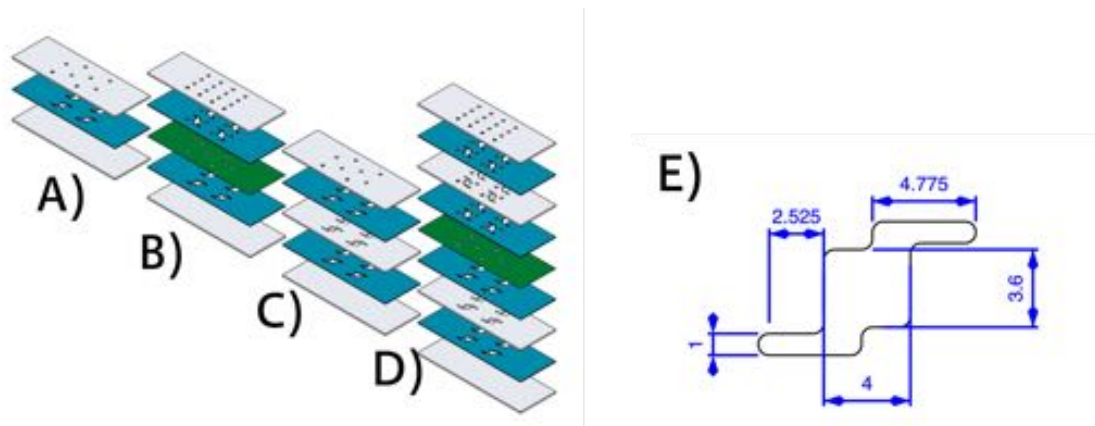
Figure 14: Chip design for determining vapor transfer rate. Material: glass (grey), membrane (green), PDMS and pressure sensitive double-sided adhesive tapes (turquoise), A) single channel design B) two channel membrane design C) big channel design D) two big channel membrane design E) dimensions of channels (total length of channel wall = 29.925 mm)

To determine the medium vapor transfer rate through the pressure sensitive double-sided adhesive tapes in comparison to PDMS chips were build according to Figure 14 A. To compare different chips designs chips has been built according to Figure 14 B for a two channel membrane design (Whatman® Cyclopore® polycarbonate membranes Sigma-Aldrich) , to Figure 14 C for a big channel design by an extra layer of glass and according to Figure 14 D for two big channel designs (by glass) with a membrane (Whatman® Cyclopore® polycarbonate membranes Sigma-Aldrich) in between.

medium vapor transfer rate $[\frac{mg}{mm^2h}]$			
by material		by design	
PDMS	$20.66 \cdot 10^{-6}$	ARcare 90106 two channel membrane design	$2.14 \cdot 10^{-6}$
ARcare 90445	0	ARcare 90880 two channel membrane design	$9.63 \cdot 10^{-6}$
ARcare 90106	$7.49 \cdot 10^{-6}$	ARcare 90880 big channel design	$6.42 \cdot 10^{-6}$
ARcare 90880	$8.56 \cdot 10^{-6}$	ARcare 90880 two big channel membrane design	$8.91 \cdot 10^{-6}$

Table 5: medium vapor transfer rate of cell culture medium for 24h at 36.5ºC through different materials within the same design (left column see Fig. 14A) with different designs (right column see Fig. 14 B-D)

The evaporation in a microfluidic system is influenced by many factors as time, temperature, perfusion and applied pressure as well as chosen materials and bonding technics of those. In regards of engineering the influence of the choose material and the bonding technic must be considered. To get an understanding how this two parameters influence a the vapor impermeability of the chip the medium vapor transfer rate is measured for different materials and different designs (more details see Table 5).
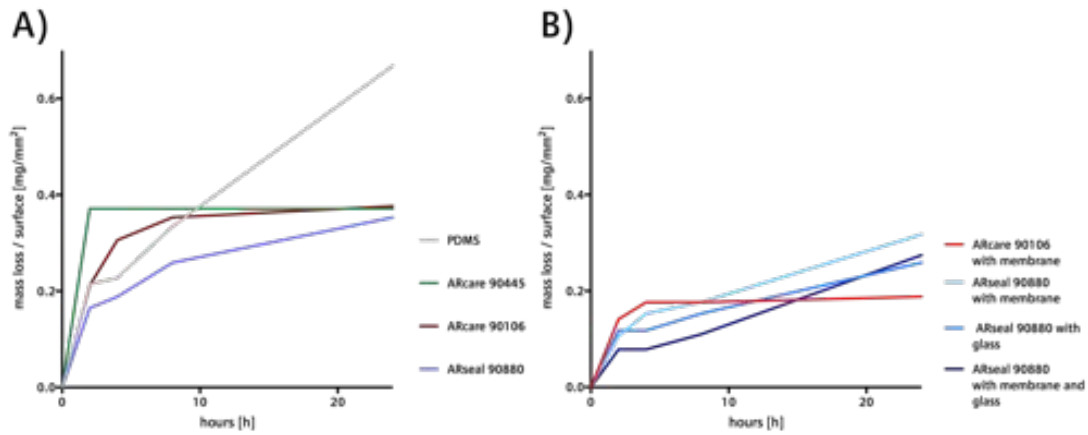
Figure 15: Evaporation of cell culture medium for 24h at 36.5ºC A) through different materials within the same design B) with different designs (see Fig. 14)

As seen in Figure 15 A, a chip build out of PDMS has a significantly higher loss of medium (0.67 mg/mm² after 24h) compared to ARcare 90445 (0.37 mg/mm² after 24h). ARcare 90106 (0.38 mg/mm² after 24h) and ARseal 90880 (0.35 mg/mm² after 24h). To determine the medium vapor transfer rate the mass loss per area at 24h was subtracted by the value at 2h (to exclude the rapid changes with in the first 2h) and divided by 20 which results in $\frac{mg}{mm^2h}$. When the rate of medium transfer through the boundaries is evaluated between 2 and 24 h (see table 5), the rate through PDMS is nearly 3 times higher compared to the adhesive tapes. There was no medium vapor transfer rate through ARcare 90445. The reason for this can be the manual assembly of the chips where the pressure for bonding is applied by hand. Different tight bondings result in sealing strength and therefore in different vapor transfer rates. Nevertheless all the adhesive tapes have a very low permeability to medium vapor which can be go down to 0. By using different chips design, which means to incorporate different layer of materials as membranes or glass the vapor rate can differ from $2.14 \cdot 10^{-6}$ up to $9.63 \cdot 10^{-6}$ $\frac{mg}{mm^2h}$, only half of the measured $20.66 \cdot 10^{-6}$ $\frac{mg}{mm^2h}$ of PDMS. Taking the amounts of evaporated medium per area in account ARcare 90106 with an incorporated membrane has only 0.19 mg/mm² after 24h compared with bonded to glass with ARcare 90106 0.38 mg/mm² after 24h. This could be caused as well by the manual assembly of the chips as mentioned before. It can be summarized that the pressure sensitive adhesive tapes provide a much better barrier to medium vapor compared to PDMS. The rate is heavily influenced by the manual assembling of the chip. Unfortunately the permeability to water vapor of PDMS can cause affect on static no-flow, osmolarity-sensitive experiments and cause cell death from bubble propagation [39]. By incorporating media baths or sacrificial liquid reservoirs, bubbles can be avoided or through a humidified environment the vapor rate can be reduced. By using pressure sensitive adhesive tapes a more controllable environment in regards of humidity can be established as compared to PDMS where small channels with a high surface to volume ratio have drastically evaporation.
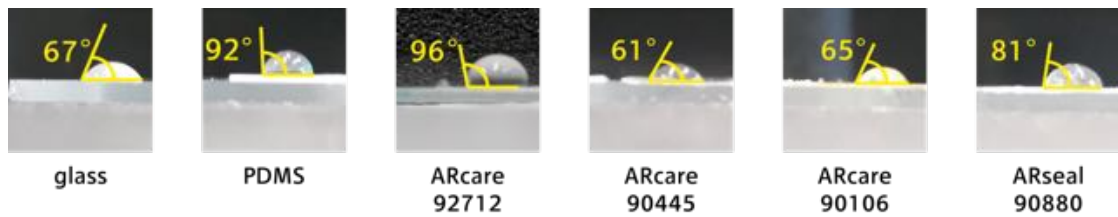
Figure 16: Hydrophilicity by contact angle of water

To evaluate hydrophobic properties of in comparison to standard materials, the pressure sensitive adhesives as well as glass and PDMS were analyzed by the contact angle of water.

Glass with an angle of 67° has neither hydrophobic nor hydrophilic characteristics and give proteins a proper surface to adhere (see Figure 16). PDMS is hydrophobic with a contact angle of 92°, but due to the surface properties cells are not able to adhere. Often as a material as a choice of chips, the PDMS surface is treated or other materials are incorporated as basal supports. Compared to those materials ARcare 92712 and ARseal 90880 are in the range of PDMS. ARcare 90445 and ARcare 90106 in the range of glass.

Bubble formation causes inappropriate perfusion of the chip and can harm the cells by an overexposure of oxygen or causing unphysiological shear stress to the cells within the device [39]. Therefore hydrophilic surfaces within a device helps to perfuse the chip proper and moderate hydrophily surfaces eases the cell to adhere to the substrate [70]. The adhesive layer represents 74% for ARcare92712, 69% for ARcare 90445, 82% for ARcare 90106 and 64% for ARseal 90880 of the lateral channel walls. Therefore the hydrophily or hydrophobic characteristics of those layers influences the fluidic behavior inside the chip. By determining the contact angle of a distilled water droplet the degree of hydrophilic (low contact angle under 90°, water spreads across the surface) or hydrophobic (high contact angle over 90°) behavior can be identified and compared. Therefore the adhesive of AS-110 acrylic medical grade adhesive of ARcare 90445 (69% of the total thickness) has the highest degree of hydrophilicity. In regards of good channel materials ARcare 90445 shows the best properties to establish easy to fill and easy to perfuse devices. In the same range the MA-69 acrylic hybrid medical grade adhesive of the ARcare 90106 behaves. Also based on acryl the adhesive of ARcare 92712 is more hydrophobic which can because by a different composition. The hydrophilicity of ARseal 90880 with SR-26 silicone adhesive lies between ARcare 92712 and ARcare 90445. Both biocompatible silicon and biocompatible acryl can be produced with hydrophily or hydrophobic properties [71]. Thereby the determination of the hydrophilicity of the adhesives can only be taken for the materials shown here. The different degree of hydrophilicity can be used to tune the flow behavior within the chip.
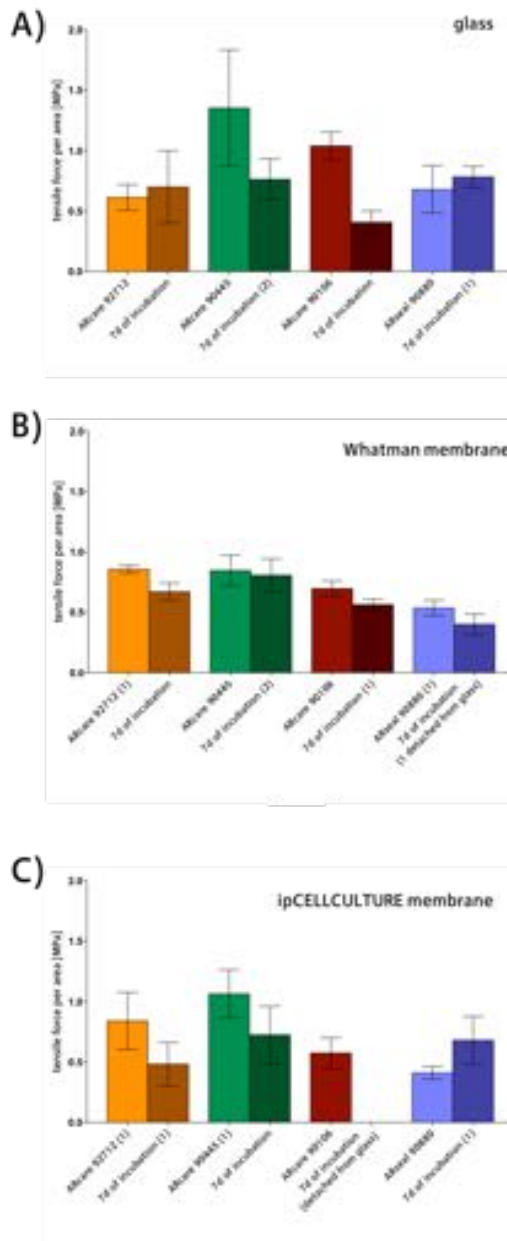
Figure 17: Maximum strength for tensile strain for the bonding between adhesive tapes an glass (A), and between adhesive tapes and the Whatman membrane (B) between adhesive tapes and the ipCELLCULTURE membrane (C) evaluated directly after bonding and after 7 days under celll culter conditions (incubator).

One of the most important steps during the manufacturing of chips is bonding different layers and structures, frequently out of different materials together. Therefore a sample of each adhesive tape (1 cm^2) is bonded between two glass slides. The samples are mounted in a 3d printed adapter to apply tensile or shear stress on the sample.

The incubation of the lab-on-a-chip can drastically influence the bonding ability. For PDMS the

presence of humidity can decrease the bonding ability or even worse cancel it [72]. Therefore the tensile forces of the adhesives is evaluated directly after bonding and after 7 day in a normal incubation environment for cell cultures. This environment has constant 37° C and a high humidity. For PDMS the presence of humidity can decrease the bonding ability or even worse cancel it [72]. The period of 7 days was chosen in regards of the final TEER experiment which will be conducted over 7 days.

The same phenomenon can be observed here as well (see Figure 17) that after 7 days of incubation (except the combination of glass with ARcare 92712 and ARseal 90880 with glass and the combination ARseal 90880 with the ipCELLCULTURE membrane) the bonding strength is reduced. For ARcare 90106 with the ipCELLCULTURE membrane (see Figure 17 C) the 7 days of incubation can cause a detachment, compared with the 573 kPa strong adhesion directly after bonding. In Figure 17 A the tensile strength of ARcare 90106 is reduced by 61% (from 1.04 MPa to 0.41 MPa) through the 7 days of incubation. The bonding strength of ARcare 90445 is reduced from 1.35 MPa to 0.76 MPA (44%). Undefinably the adhesion was increased through incubation for ARcare 92712 by 15% (from 0.61 MPa to 0.7 MPa) and ARseal 90880 by 15% (from 0.67 MPa to 0.78 MPa).

The differences between Figure 17 B and C are caused by the different materials of the membranes (Nucleopore out of polycarbonate and ipCELLCULTURE out of polyester) as well as the different surfaces treatments of those.

Taking the big influence of incubation of the chips in account, the bonding strength after 7 days should be rated. For all four scenarios in Figure 17 ARcare 90445 shows the best bonding behavior before and after incubation. A reason for the lower strength of ARcare 90106 and ARseal 90880 could be that, during cutting and peeling off, the adhesive layer forms embossments at the edges of the structure (see Figure 12). Those embossments causes a rough surface where the adhesives do not bond uniform to the sample. Therefor the total area of bonding is decreased and the tensile strength of the sample is weaker (see Figure 17 B and C). Comparing Figure 17 A with B and C the bonding of the membrane represents the weakest part of the chip. ARcare 90445 is rated as the material with the best bonding properties (0.76 MPa to glass, 0.72 MPa to ipCELLCULTRUE membrane and 0.81 MPa to Nuclepore membranes after 7 days of incubation) compared to the other adhesive tapes.

As observed for the tensile strength ARcare 90445 has the highest shear strength as well for bonding to glass and for bonding to ipCELLCULTURE membrane (see Figure 18).
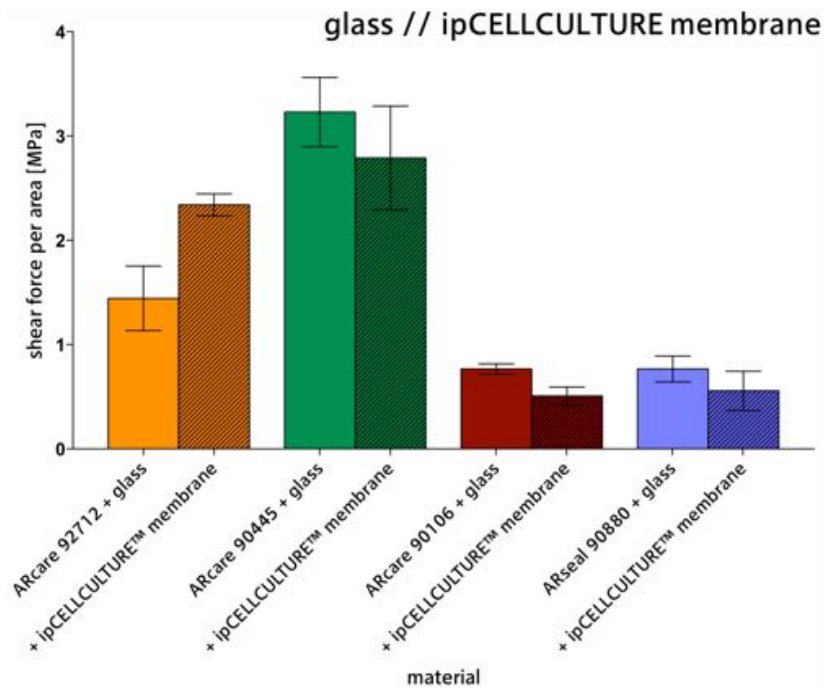
Figure 18: Shear strength of the bonding between the adhesive tapes and glass as well as the ipCELLCULTURE membranes. Data bars are mean values ± SD for n = 3. Number in brackets indicates amount of samples where the glass broke before the adhesive tape detached, the values are incluede because the tapes can handle this force.

A comparison of the measured values of this study with values in literature is not possible. All values found in literature for several materials are always chip design specific, which means that other authors only reported how much pressure their chips can handle. There are no values normed of the area of bonding.

To evaluate optical properties the absorption spectrum and the autofluorocence was measured.
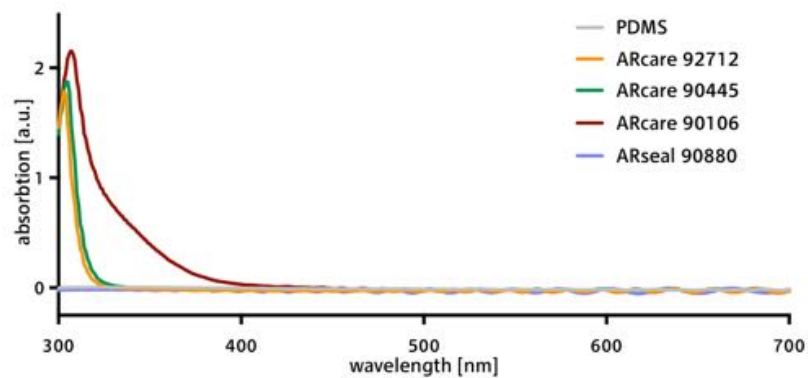

Figure 19: Absorbance of PDMS, ARcare 92712, ARcare 90445, ARcare 90106 and ARseal 90880

PDMS shows no absorption as well as ARseal 90880 in the spectrum between 300-700 nm (see

Figure 19) . In the range of 300-350 nm ARcare 92712, ARcare 90445 and ARcare 90106 shows absorption of light. This is caused by the polyester film as a carrier material. Optical inspection the MA-69 acrylic hybrid medical grade adhesive appears yellow, which contributes to the absorption peak up to 400 nm of ARcare 90106. Most staining are in the area above 350 nm. There should be no great influence on any staining procedures or on other procedures above a wavelength of 350 nm.

The method of choice for evaluating cell-based lab-on-a-chip is using fluorescence imaging. Therefore materials should not have any autofluorescence.
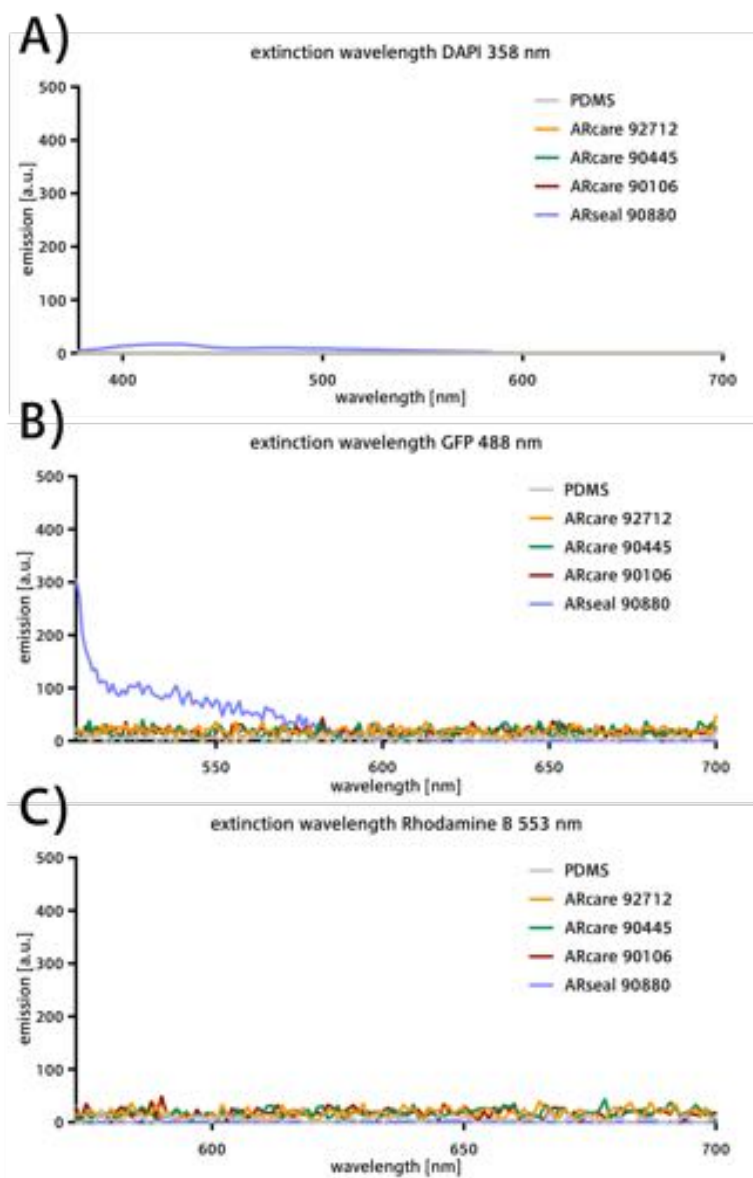

Figure 20: Fluorescence spectra of PDMS and pressure sensitive adhesive at excitation wavelentgh of A) 358 nm, B) 488 nm and C) 553 nm

The DNA-specific probe DAPI (4´,6-diamidino-2-phenylin-dole) with an excitation wave length of 358 nm is commonly used for flow cytometry, chromosome staining, DNA visualization and quantitation in histochemistry and biochemistry [73]. Therefore the emission spectrum of the material at 358 nm is evaluated. To visualized specific proteins within an cell culture photoactivatable variant of the Aequorea victoria green fluorescent protein (GFP) is used and exciting at 488 nm[74]. To stain mitochondrial membrane Rhodamine B (553 nm) is used which distributes across biological membranes in response to the electrical transmembrane potential [75]. This is a representative set of optical properties for cell staining assays within this study. Except for ARseal with an excitation at 488 nm non of the pressure sensitive double-sided adhesive tapes emits any fluorescence which offer to work with the whole spectrum of staining technics.

4.3 Assessment of biocompatibilty

The influence of chemical properties in cell adhesion and viability was assesed using live/dead as well as metabolic assays to evaluated any possible cytotoxic effects of pressures sensitive adhesives on a mammanial cell line. To quantify the influence of the adhesive layer on the cell behavior pictures of the cells with and without exposure to the adhesives were compared.

As described before the adhesive layer represents more than half of the exposed channel walls. By containing solvents, the adhesive layer can cause cytotoxicity and disturb the metabolism of cells [43]. Solvents and photoinitiator causes oxidative stress to cells [76].
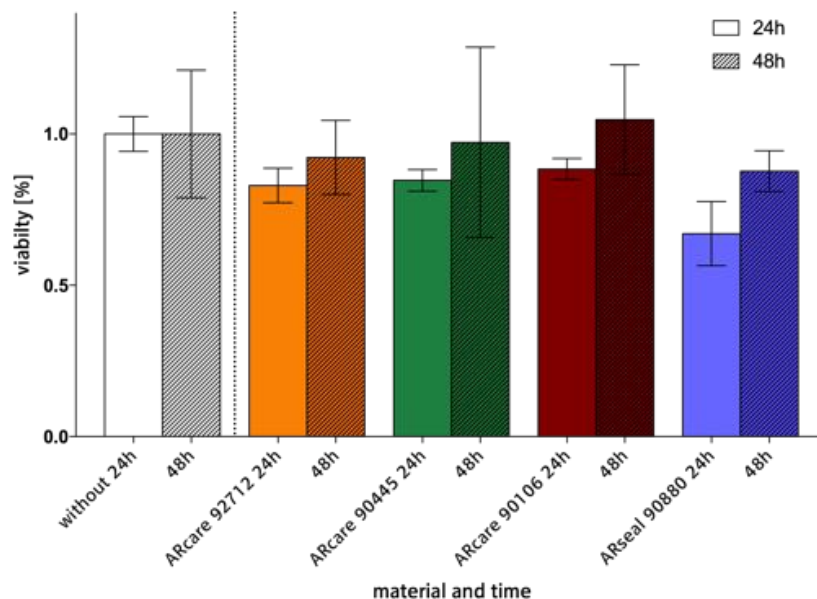

Figure 21: Viability of cells as percentage of cells without the any exposure to the adhesive layers after 24 and 48 h. Data bars are mean values ± SD for n = 3

The viability presented in Figure 21 shows that the exposure to the adhesive could cause a reduction of the viability to 67% after 24h for ARseal 90880 and reduced to 88% after 48h. It should be taken into account that standard deviation for values after 48 h is quite big, especially for ARcare 90445. The viability on the presence of ARcare 90106 increases over 48h up to 104% compared to cells with no exposure to an adhesive. Over all, all cells are vital but due to the fact that cells can't adhere to the silicone adhesive of ARseal 90880, they form spheroids (see Figure 22) what causes the lower

metabolism.

Because showing the best physical properties for fabricating membrane- and electrode-integrated cell-based lab-on-a-chip systems and causing a viability of 85% after 24h and 97% after 48h ARcare 90445 is evaluated as biocompatible material for the lab-on-a-chip system.
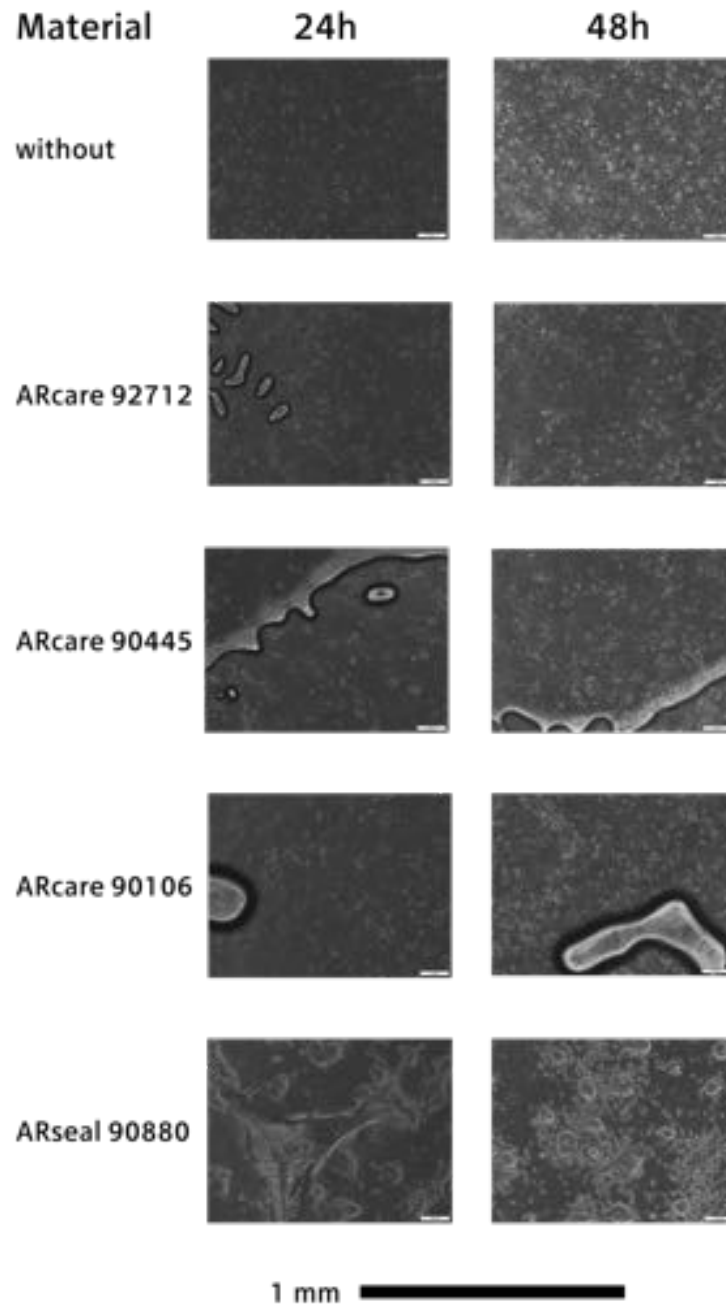

Figure 22: Cells with and without exposure to the adhesive surfaces of ARcare 92712, ARcare 90445, ARcare 90106 and ARseal 90880 after 24h and 48h

Figure 22 shows the BeWo b30 cells seeded on the adhesive surface of the different pressure sensitive double-sided adhesive tapes. After 24 h the cells adhere to the adhesive surface of ARcare 92712 and ARcare 90196 in a similar way as the well plate bottom. Cells on top of the adhesive surface of ARseal 90880 seem to have problems to adhere so they form organoids which can also be observed after 48h. Cells on the adhesive surface of ARcare 90445 seam to adhere slower but can established a closed monolayer after 48h in the same way as the cells in the presence of ARcare 92712 and 90106 do.

Figure 23 shows living cells (green) and dead cells (red). The staining of the cells is performed by adding substance to the cell medium within the well plate. By mixing the substance with medium, cell can be detached by the turbulences. The cells can't adhere strong to the adhesive layers. The cells washed away through the staining process create interrupted monolayers for all ARcare tapes. As mentioned before cells can't adhere to the adhesive layer of ARseal 90880 and form organoids. The composition of the different adhesive influences the adhesion behavior. The hydrophilicity should not influence the adhesion behavior, because cells adhere to ARcare 92712 (contact angle 91º) and to ARcare 90445 (61º) but not to ARseal 90880 (81 º). In the presence of ARcare 90106 cells form a confluent monolayer after 48h but also died more compared to the other adhesive layers. Overall the presence of the adhesive layers did not cause drastically dying of cells.
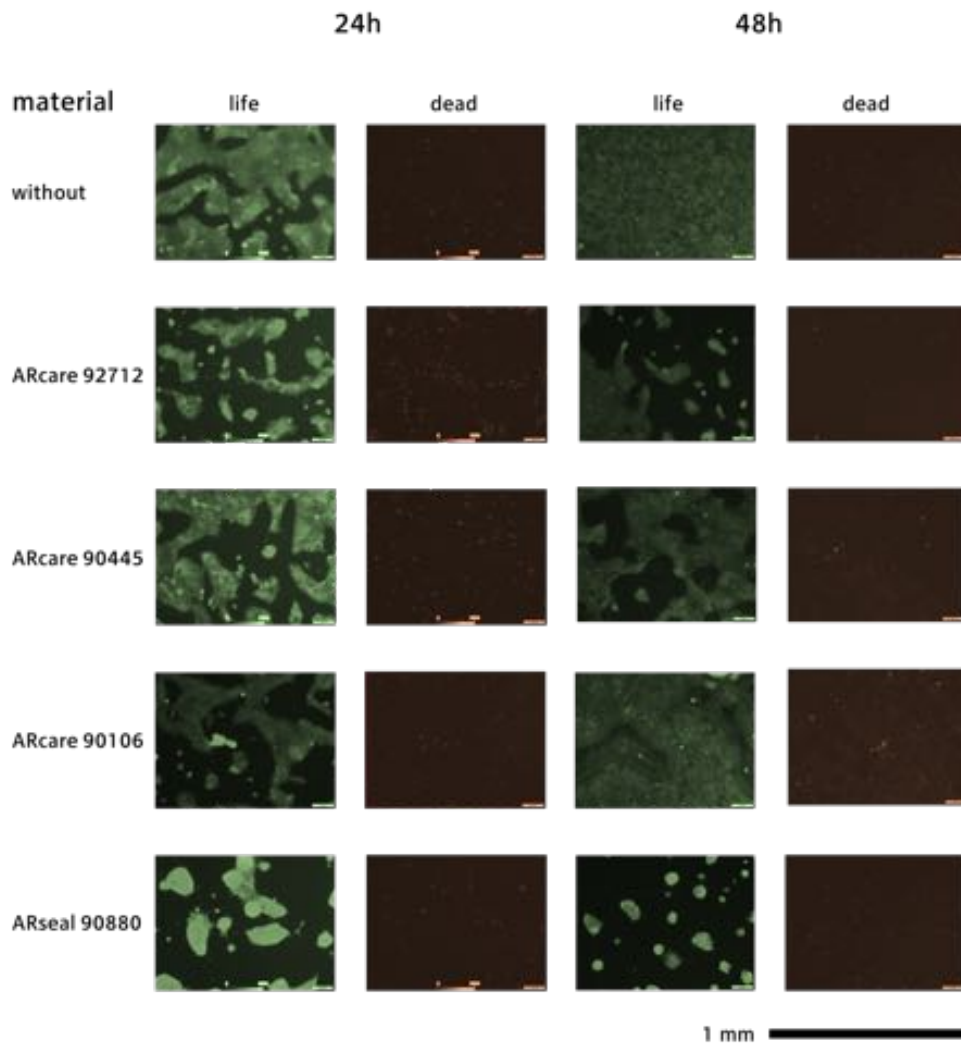
Figure 23: Living (green) and dead (red) cells in the present of the adhesive surfaces of of ARcare 92712, ARcare 90445, ARcare 90106 and ARseal 90880 after 24h and 48h

To analyze which membrane is suitable for cell culturing as well as has the best optical properties for imaging cell were seeded on different membranes with and without collagen treatments.
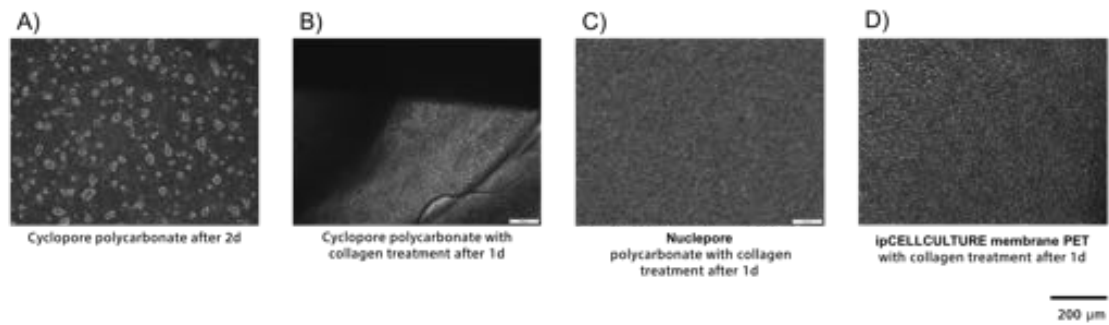
Figure 24: BeWo b30 cells on different polymer membranes A) cyclopore polycarbonate B) cyclopore polycarbonate with collagen treatment C) nuclepore polycarbonate with collagen treatment and D) ipCELLCULTURE pet membrane with collagen treatment

The membrane in the cell-based lab-on-a-chip system represents the tissue interface on which the cells adhere. With being the only material of the chip in direct physical contact with cells, the properties in regards of cell culturing are very important. By observing the chip with the help of a microscope a transparent membrane is advantageous.

As seen in Figure 24 A cells couldn't attach to the untreated membrane compared to the collagen treated in B. The polycarbonate membrane under C provides a better environment for cells by being produced for cell culturing. Used in other cell-based lab-on-a-chip system [77] the ipCELLCULTURE membrane is already established and has the best transparency (see Figure 24 D). Therefor the ip-CELLCULTURE membranes are incorporated in the the membrane in the cell-based lab-on-a-chip system.

To determine which amount of cells seeded is suitable to establish a confluent monolayer as fast as possible different densities were seeded in wells. The amount 12,5 k, 25k and 50k cells per cm^2 is to small to establish monolayers after 3 days. The amount of 200k cells per cm^2 is to high so that not all cells can adhere to the basal support which causes dying of those. The density of 100k cells per cm^2 which is also reported in other studies [29] is suitable to have a confluent monolayer within 1 day. A fast established monolayer without residual cells not adhered to the membrane is needed to conduct a proper TEER measurement.
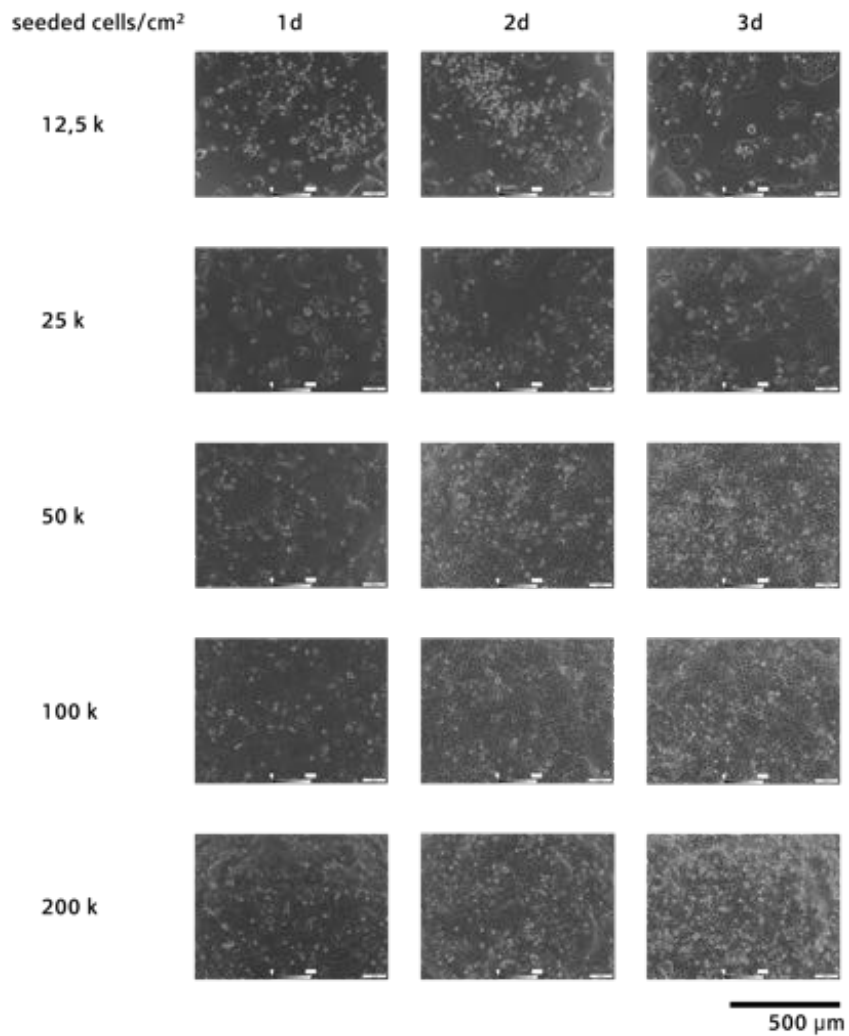
Figure 25: Different density of seeded BeWo b30 cells after 1,2 and 3 days

4.4 Proof of concept on chip TEER measurement

As proof of concept for the feasibility of biomedical adhesives a lab-on-a-chip was assembled out of glass, the ipCELLCULTURE membrane and ARcare 90445 and a TEER measurement was carried out over 7 days. To enlarge the channels as shown in Figure 26 intermedia layers of glass were incorporated. By a channel volume of 150 µl (see Table 6) and flow of 2 µl/min the shear force of 0.0006 Dyn on the cells is negligible.
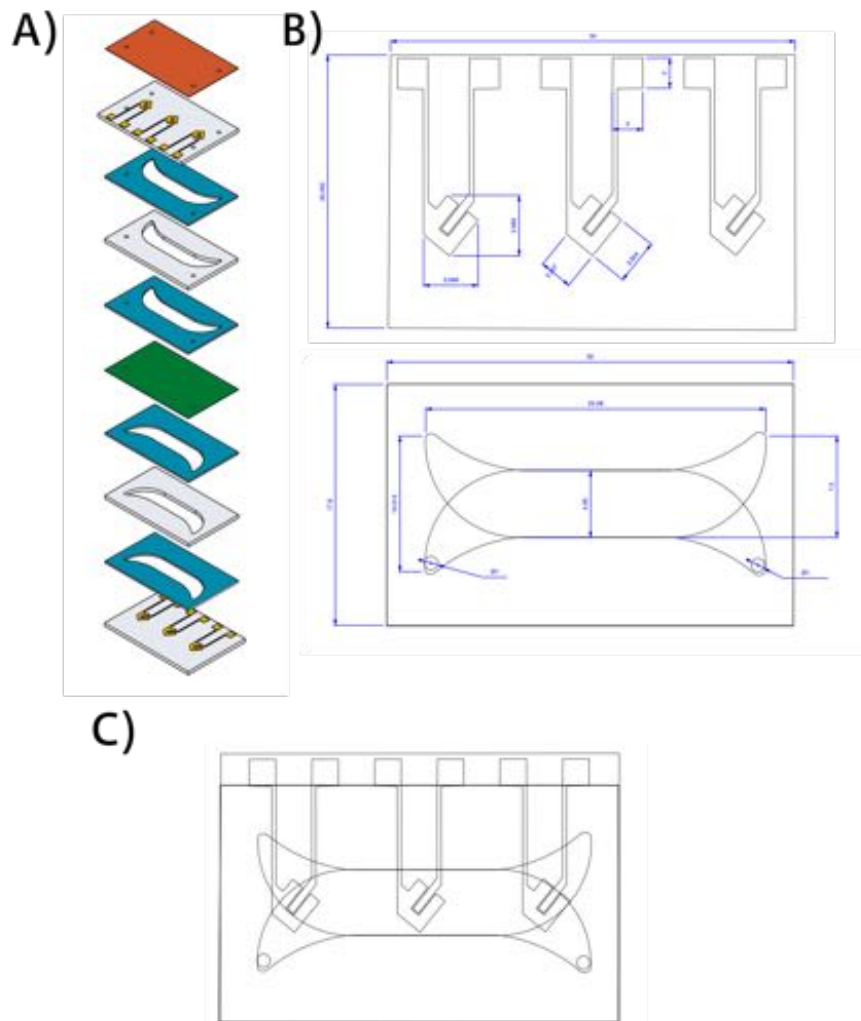
Figure 26: TEER Chip design A) composition: glass (grey) with and without electrodes (yellow), ARcare 90445 (turquoise), ipCELLCULTURE™ membrane (green) and ARcare 90106 as sealing (red) B) dimensions of the electrodes and the symmetric channels C) electrode arrangement within the channels

The chip was build easily within 3h as described in Figure 26 A. The electrode integrated glass slides were already in stock Figure 26 B. The chip stayed leakage free for 7 days in the interface shown in Figure 11 and was perfused at the second day with 2 µl/min maintained at 37⁰. The seeded BeWo b30 cells adhered after 24h to the collagen treated membrane (see Figure 27) until day 7. Through the establishment of a monolayer of BeWo b30 cells the resistance of the cells and the membrane increases up to 0.12 kΩ and 0.17 kΩ at day 2 (see Figure 27 A). The TEER increases significantly with developing of tight junctions between the cells. This can be observed at day 2 where the slope of the TEER measurement increases and a confluent monolayer was established. Since confluence was achieved at day 2 flow was initiated to remove waste products of the cell metabolism.

channel hight [mm]	1,26
channel width [mm]	4,95
channel length (straight part) [mm]	11,08
membrane surface [mm^2]	119,5
length of channel wall [mm]	60,7
volume of channel [µl]	150
cells per ml needed for seeding	80k

Table 6: TEER chip properties

By pumping only 2 µl/min which is only 1.3 % of the total channel volume, therefore the total channel volume is replaced every 77 minutes the effect of the perfusion is negligible. The TEER increases significantly with developing of tight junctions between the cells. At day 7 the resistance over the membrane with the cell monolayer is 1.517 kΩ, a rate of 0.27 kΩ/day from day 2 to day 7. The state after 7 days is considered as a tight barrier. To validate that the over all trend in the TEER measurement was caused by the barrier properties and not by a sensor drift through electrode delamination, the BeWo b30 cells were detached by trypsin from the ipCELLCULTURE membrane. As Figure 27 B shows the monolayer of the cells was partly destroyed through the use of trypsin and the resistance reduced to 0.832 kΩ. Therefore the relative TEER value caused by the tight cell barrier was 0.685 kΩ and the sensor drift 0.832 kΩ. As the picture of the cells in B after the use of trypsin illustrates not all cells detached from the membrane which could explain that the resistance was only reduced by 45%. On the whole the values of TEER measurement should be only taken as an overall trend that can be observed. In fact only a small gap, about 0.4% can cause a drop of the resistance by 80%[17]. Further more the overall geometry of the set up can have a enormous influence of measurement [17]. On account of this it is not reasonable to compare TEER values from different studies against each others [18]. For this reason it is also not acceptably to compare the values of static transwell measurements with the values of dynamic cultivation on a chip. Only trends can be compared. The trend that the slope of the TEER measurement increases after day 2 can also seen in the study of Cartwright et al where the resistance of a BeWo b30 monolayer in a transwell is measured [78] and the study of Carreira et al. to investigate the influence of polychlorinated biphenyls on the placenta barrier [79]. Both studies report different developments of the TEER value. Cartwright et al. measured increasing values over 13 days however Carreira et al. measured an decrease after 6 days for BeWo b30 cells without any influence.

Here a membrane- and electrode-integrated cell-based lab-on-a-chip system is established where cells can be cultured over 7 days and the TEER can be measured to observe the barrier properties as adhesion and tight junctions of the cell monolayer. Trypsin was used to show that the significant increase of the resistance between the two electrodes was caused by the established cell monolayer.
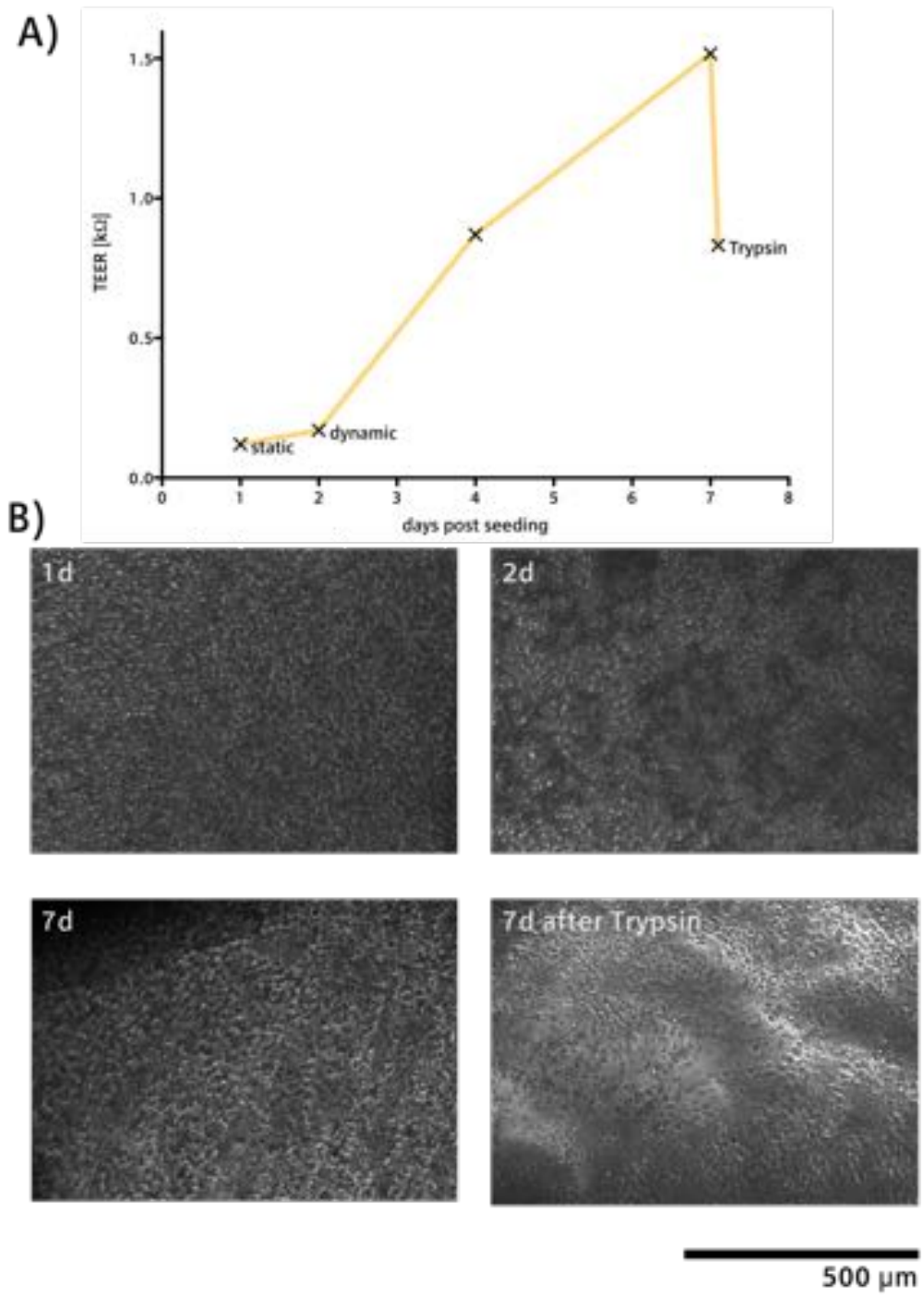
Figure 27: TEER measurement conducted in the membrane- and electrode-integrated cell-based lab-on-a-chip system A) TEER measurement over 7 days wit 0 Ohm correspond to blank membrane values of acellular scenario B) BeWO b30 cells after 1 day, 2 days and 7 days and after use of trypsin at day 7

5   Conclusion

biomedical pressure sensitive double-sided adhesive tape	ARcare 92712	ARcare 90445	ARcare 90106	ARseal 90880
cutting behavior (tolerance in µm)	**50**	**50**	75	75
Medium vapor transfer rate (in $\frac{mg}{mm^2 h}$)	-	**0**	$7.49 \cdot 10^{-6}$	$8.56 \cdot 10^{-6}$
hydrophilicity (water contact angle)	96º	**61º**	65º	81º
tensile strength (glass incubated in MPa)	0.7	0.76	0.41	**0.78**
tensile strength (ipCELLCULTURE membrane incubated in MPa)	0.48	**0.72**	0	0.68
shear force (glass in MPa)	1.44	**3.23**	0.77	0.77
shear force (ipCELLCULTURE membrane in MPa)	2.34	**2.79**	0.51	0.56
cell compatibility (ranked 1 best 4 worth)	3	**1**	2	4
cell viability after 24 h (in %)	**89**	85	88	67
cell viability after 48 h (in %)	92	97	**104**	88

Table 7: Characterization of functional biomedical adhesives (most suitable **values** are bolded)

The membrane- and electrode-integrated cell-based lab-on-a-chip system is established and an experiment over 7 days with BeWo b30 cells is carried out. By using pressure sensitive double-sided adhesive tapes the concept-to-chip time is under 3h. This rapid prototyping represents a very easy and fast adaption and manufacturing of the membrane- and electrode-integrated cell-based lab-on-a-chip system. There is no clean room needed and only a low investment in the manufacturing infrastructure is necessary. The adhesive tape ARcare 90445 shows suitable properties which withstand the experimental set up. The experimental set up is realized in a self designed and 3D-printed interface. This interface can be printed and assembled with in 2h. The manufacturing and connecting of the chip to the lab environment is suitable quick which allows really rapid prototyping and testing of those.

Through the physical characterization as described before and summarized in Table 7 the pressure sensitive double-sided adhesive tape with most suitable characteristics can be chosen. As Table 7 shows ARcare 90445 has the next to ARcare 92712 the smallest tolerance (precise structure), no

vapor rate (stable microenvironment), the highest hydrophilicity (proper flow), the highest bonding strength to the chosen ipCELLCULTURE membranes (crucial part in regards of sealing) and the best cell compatibility as well as as negligible influence of the cell viability. Further more the optical properties give no further restrictions. Therefor ARcare 90445 was chosen to build up the membrane- and electrode-integrated cell-based lab-on-a-chip system.

The valid lab-on-a-chip system can be used to study the influence of the barrier properties through nanoparticles and drugs. Beside the TEER measurement the integrated electrodes can be used to new applications as short circuit current, action potentials of electrically active cells for electrophysiology studies, which are currently lacking in the majority of micro physiological systems.

Here the proof of concept is established, further more a more precise calibration of the sensors is needed to better correlate the changes in the TEER to the barrier properties. To use the membrane- and electrode-integrated cell-based lab-on-a-chip system for several tissue interface models more cell lines needed to be studied with in the lab-on-a-chip.

The emerging technology of lab-on-a-chip systems gains more complex models with deeper insights, but there is still a lack of comparison between the models of cell-based lab-on-a-chip system [1]. They still have a deficiency in the key factors reliability, functionality and reproducibility which minimize the usability. Those systems are still academic tools focusing on modeling complex microenvironment and a lack of industrial usage [11]. Apart from the progress propagated by the microfluidic and organ on a chip community it has been taken into account that they are still models. It is worked on to create the dynamic mechanical and biochemical microenvironment to build valid artificial engineering organs and not the real organ [19].

Here we demonstrated a validated membrane- and electrode-integrated cell-based lab-on-a-chip system which will be used to gain understanding of the human body as precise as possible to ensure progress in medicine and drug research.

References

[1] Zhang, B. & Radisic, M. Organ-on-a-chip devices advance to market. *Lab Chip* **17**, 2395–2420 (2017).

[2] Abbott, A. Cell culture: biology's new dimension. *Nature* **424**, 870–2 (2003).

[3] Paul, S. M. *et al.* How to improve r&d productivity: the pharmaceutical industry's grand challenge. *Nat Rev Drug Discov* **9**, 203–14 (2010).

[4] Greek, R. & Menache, A. Systematic reviews of animal models: methodology versus epistemology. *Int J Med Sci* **10**, 206–21 (2013).

[5] Hartung, T. Opinion versus evidence for the need to move away from animal testing. *ALTEX* **34**, 193–200 (2017).

[6] Mouse Genome Sequencing Consortium *et al.* Initial sequencing and comparative analysis of the mouse genome. *Nature* **420**, 520–62 (2002).

[7] Fernandez, M. L. & Volek, J. S. Guinea pigs: a suitable animal model to study lipoprotein metabolism, atherosclerosis and inflammation. *Nutr Metab (Lond)* **3**, 17 (2006).

[8] Benirschke, K. & Driscoll, S. G. *The pathology of the human placenta* (Springer-Verlag, Berlin, 1967).

[9] Mak, I. W., Evaniew, N. & Ghert, M. Lost in translation: animal models and clinical trials in cancer treatment. *American Journal of Translational Research* **6**, 114–118 (2014). URL http://www.ncbi.nlm.nih.gov/pmc/articles/PMC3902221/.

[10] DiMasi, J. A., Grabowski, H. G. & Hansen, R. W. Innovation in the pharmaceutical industry: New estimates of r&d costs. *J Health Econ* **47**, 20–33 (2016).

[11] Liu, Y., Gill, E. & Shery Huang, Y. Y. Microfluidic on-chip biomimicry for 3d cell culture: a fit-for-purpose investigation from the end user standpoint. *Future Sci OA* **3**, FSO173 (2017).

[12] Huh, D., Hamilton, G. A. & Ingber, D. E. From 3d cell culture to organs-on-chips. *Trends Cell Biol* **21**, 745–54 (2011).

[13] Whitesides, G. M. The origins and the future of microfluidics. *Nature* **442**, 368–73 (2006).

[14] Pisanic, I., Thomas R., Blackwell, J. D., Shubayev, V. I., Finones, R. R. & Jin, S. Nanotoxicity of iron oxide nanoparticle internalization in growing neurons. *Biomaterials* **28**, 2572–2581 (2007).

[15] Boncler, M., Rozalski, M., Krajewska, U., Podsedek, A. & Watala, C. Comparison of prestoblue and mtt assays of cellular viability in the assessment of anti-proliferative effects of plant extracts on human endothelial cells. *J. Pharmacol. Toxicol. Methods* **69**, 9–16 (2014).

[16] Fang, Y., Li, G. & Ferrie, A. M. Non-invasive optical biosensor for assaying endogenous g protein-coupled receptors in adherent cells. *J Pharmacol Toxicol Methods* **55**, 314–22 (2007).

[17] Odijk, M. *et al.* Measuring direct current trans-epithelial electrical resistance in organ-on-a-chip microsystems. *Lab Chip* **15**, 745–52 (2015).

[18] Henry, O. Y. F. *et al.* Organs-on-chips with integrated electrodes for trans-epithelial electrical resistance (teer) measurements of human epithelial barrier function. *Lab Chip* **17**, 2264–2271 (2017).

[19] Zheng, F. *et al.* Organ-on-a-chip systems: Microengineering to biomimic living systems. *Small* **12**, 2253–82 (2016).

[20] Huh, D. *et al.* Reconstituting organ-level lung functions on a chip. *Science* **328**, 1662–8 (2010).

[21] Lee, S.-A. *et al.* Spheroid-based three-dimensional liver-on-a-chip to investigate hepatocyte-hepatic stellate cell interactions and flow effects. *Lab Chip* **13**, 3529–37 (2013).

[22] Huh, D. *et al.* Acoustically detectable cellular-level lung injury induced by fluid mechanical stresses in microfluidic airway systems. *Proc Natl Acad Sci U S A* **104**, 18886–91 (2007).

[23] Ho, C.-T., Lin, R.-Z., Chang, W.-Y., Chang, H.-Y. & Liu, C.-H. Rapid heterogeneous liver-cell on-chip patterning via the enhanced field-induced dielectrophoresis trap. *Lab Chip* **6**, 724–34 (2006).

[24] Lee, J. S. *et al.* Placenta-on-a-chip: a novel platform to study the biology of the human placenta. *J Matern Fetal Neonatal Med* **29**, 1046–54 (2016).

[25] Gude, N. M., Roberts, C. T., Kalionis, B. & King, R. G. Growth and function of the normal human placenta. *Thrombosis Research* **114**, 397–407 (2004). URL http://www.sciencedirect.com/science/article/pii/S0049384804003421.

[26] Jones, H. N., Powell, T. L. & Jansson, T. Regulation of placental nutrient transport –a review. *Placenta* **28**, 763–774 (2007). URL http://www.sciencedirect.com/science/article/pii/S0143400407001130.

[27] Lager, S. & Powell, T. L. Regulation of nutrient transport across the placenta. *J Pregnancy* **2012**, 179827 (2012).

[28] Abbas, Y. *et al.* A microfluidics assay to study invasion of human placental trophoblast cells. *J R Soc Interface* **14** (2017).

[29] Rothbauer, M. *et al.* A comparative study of five physiological key parameters between four different human trophoblast-derived cell lines. *Sci Rep* **7**, 5892 (2017).

[30] Strohmer, H. *et al.* Hypoxia downregulates continuous and interleukin-1-induced expression of human chorionic gonadotropin in choriocarcinoma cells. *Placenta* **18**, 597–604 (1997). URL http://www.sciencedirect.com/science/article/pii/0143400477900169.

[31] Sivasubramaniyam, T. *et al.* Where polarity meets fusion: role of par6 in trophoblast differentiation during placental development and preeclampsia. *Endocrinology* **154**, 1296–309 (2013).

[32] Wick, P. *et al.* Barrier capacity of human placenta for nanosized materials. *Environ Health Perspect* **118**, 432–6 (2010).

[33] Miura, S., Sato, K., Kato-Negishi, M., Teshima, T. & Takeuchi, S. Fluid shear triggers microvilli formation via mechanosensitive activation of trpv6. *Nat Commun* **6**, 8871 (2015).

[34] Burton, G. J., Woods, A. W., Jauniaux, E. & Kingdom, J. C. P. Rheological and physiological consequences of conversion of the maternal spiral arteries for uteroplacental blood flow during human pregnancy. *Placenta* **30**, 473–82 (2009).

[35] Lecarpentier, E. *et al.* Computational fluid dynamic simulations of maternal circulation: Wall shear stress in the human placenta and its biological implications. *PLoS One* **11**, e0147262 (2016).

[36] Plitman Mayo, R., Charnock-Jones, D. S., Burton, G. J. & Oyen, M. L. Three-dimensional modeling of human placental terminal villi. *Placenta* **43**, 54–60 (2016).

[37] Esch, E. W., Bahinski, A. & Huh, D. Organs-on-chips at the frontiers of drug discovery. *Nat Rev Drug Discov* **14**, 248–60 (2015).

[38] Günther, A. *et al.* A microfluidic platform for probing small artery structure and function. *Lab Chip* **10**, 2341–9 (2010).

[39] Berthier, E., Young, E. W. K. & Beebe, D. Engineers are from pdms-land, biologists are from polystyrenia. *Lab Chip* **12**, 1224–37 (2012).

[40] Waldbaur, A., Rapp, H., Laenge, K. & Rapp, B. E. Let there be chip-towards rapid prototyping of microfluidic devices: one-step manufacturing processes. *Anal. Methods* **3**, 2681–2716 (2011).

[41] Becker, H. One size fits all? *Lab Chip* **10**, 1894–1897 (2010). URL http://dx.doi.org/10.1039/C005380P.

[42] Temiz, Y., Lovchik, R. D., Kaigala, G. V. & Delamarche, E. Lab-on-a-chip devices: How to close and plug the lab? *Microelectronic Engineering* **132**, 156 – 175 (2015). URL http://www.sciencedirect.com/science/article/pii/S0167931714004456. Micro and Nanofabrication Breakthroughs for Electronics, MEMS and Life Sciences.

[43] Chen, T. *et al.* A drug-compatible and temperature-controlled microfluidic device for live-cell imaging. *Open Biology* **6**, 160156 (2016). URL http://www.ncbi.nlm.nih.gov/pmc/articles/PMC5008015/.

[44] Wang, J. *et al.* Towards disposable lab-on-a-chip: poly(methylmethacrylate) microchip electrophoresis device with electrochemical detection. *Electrophoresis* **23**, 596–601 (2002).

[45] Lee, G. B., Chen, S. H., Huang, G. R., Sung, W. C. & Lin, Y. H. Microfabricated plastic chips by hot embossing methods and their applications for dna separation and detection. *Sens. Actuator B-Chem.* **75**, 142–148 (2001).

[46] Piruska, A. *et al.* The autofluorescence of plastic materials and chips measured under laser irradiation. *Lab Chip* **5**, 1348–1354 (2005).

[47] Johnson, T. J., Ross, D. & Locascio, L. E. Rapid microfluidic mixing. *Anal. Chem.* **74**, 45–51 (2002).

[48] Yang, J. N. *et al.* High sensitivity pcr assay in plastic micro reactors. *Lab Chip* **2**, 179–187 (2002).

[49] Rhee, S. W. *et al.* Patterned cell culture inside microfluidic devices. *Lab Chip* **5**, 102–107 (2005).

[50] Taylor, A. M. *et al.* Microfluidic multicompartment device for neuroscience research. *Langmuir* **19**, 1551–1556 (2003).

[51] Yang, W. W., Lu, Y. C., Xiang, Z. Y. & Luo, G. S. Monodispersed microcapsules enclosing ionic liquid of 1-butyl-3-methylimidazolium hexafluorophosphate. *React. Funct. Polym.* **67**, 81–86 (2007).

[52] Astorga-Wells, J., Jornvall, H. & Bergman, T. A microfluidic electrocapture device in sample preparation for protein analysis by maldi mass spectrometry. *Anal. Chem.* **75**, 5213–5219 (2003).

[53] Wu, Z. Y., Xanthopoulos, N., Reymond, F., Rossier, J. S. & Girault, H. H. Polymer microchips bonded by o-2-plasma activation. *Electrophoresis* **23**, 782–790 (2002).

[54] Irawan, R., Swaminathan, S., Aparajita, P. & Tjin, S. C. Fabrication and performance testing of disposable micropump suitable for microfluidic chip. In *2006 International Conference on Biomedical and Pharmaceutical Engineering*, 252–255 (2006).

[55] Kim, D. S., Lee, S. H., Ahn, C. H., Lee, J. Y. & Kwon, T. H. Disposable integrated microfluidic biochip for blood typing by plastic microinjection moulding. *Lab Chip* **6**, 794–802 (2006).

[56] Vengasandra, S., Cai, Y., Grewell, D., Shinar, J. & Shinar, R. Polypropylene cd-organic light-emitting diode biosensing platform. *Lab Chip* **10**, 1051–1056 (2010).

[57] Janmey, P. A., Winer, J. P., Murray, M. E. & Wen, Q. The hard life of soft cells. *Cell Motil Cytoskeleton* **66**, 597–605 (2009).

[58] Domansky, K. *et al.* Clear castable polyurethane elastomer for fabrication of microfluidic devices. *Lab Chip* **13**, 3956–64 (2013).

[59] Borysiak, M. D., Yuferova, E. & Posner, J. D. Simple, low-cost styrene-ethylene/butylene-styrene microdevices for electrokinetic applications. *Anal Chem* **85**, 11700–4 (2013).

[60] Guillemette, M. D., Roy, E., Auger, F. A. & Veres, T. Rapid isothermal substrate microfabrication of a biocompatible thermoplastic elastomer for cellular contact guidance. *Acta Biomater* **7**, 2492–8 (2011).

[61] Mondrinos, M. J., Yi, Y.-S., Wu, N.-K., Ding, X. & Huh, D. Native extracellular matrix-derived semipermeable, optically transparent, and inexpensive membrane inserts for microfluidic cell culture. *Lab Chip* **17**, 3146–3158 (2017).

[62] de Jong, J., Lammertink, R. G. H. & Wessling, M. Membranes and microfluidics: a review. *Lab Chip* **6**, 1125–1139 (2006).

[63] Benyo, D. F., Miles, T. M. & Conrad, K. P. Hypoxia stimulates cytokine production by villous explants from the human placenta. *J Clin Endocrinol Metab* **82**, 1582–8 (1997).

[64] Sabourin, D., Snakenborg, D. & Dufva, M. Interconnection blocks: a method for providing reusable, rapid, multiple, aligned and planar microfluidic interconnections. *J. Micromech. Microeng.* **19** (2009).

[65] Christensen, A. M., Chang-Yen, D. A. & Gale, B. K. Characterization of interconnects used in pdms microfluidic systems. *J. Micromech. Microeng.* **15**, 928–934 (2005).

[66] Scott, A., Au, A. K., Vinckenbosch, E. & Folch, A. A microfluidic d-subminiature connector. *Lab Chip* **13**, 2036–2039 (2013).

[67] Perozziello, G., Bundgaard, F. & Geschke, O. Fluidic interconnections for microfluidic systems: A new integrated fluidic interconnection allowing plug 'n' play functionality. *Sens. Actuator B-Chem.* **130**, 947–953 (2008).

[68] Saarela, V. *et al.* Re-usable multi-inlet pdms fluidic connector. *Sens. Actuator B-Chem.* **114**, 552–557 (2006).

[69] Atencia, J. *et al.* Magnetic connectors for microfluidic applications. *Lab Chip* **10**, 246–249 (2010).

[70] Arima, Y. & Iwata, H. Effect of wettability and surface functional groups on protein adsorption and cell adhesion using well-defined mixed self-assembled monolayers. *Biomaterials* **28**, 3074–82 (2007).

[71] Abela-Formanek, C., Amon, M., Kahraman, G., Schauersberger, J. & Dunavoelgyi, R. Biocompatibility of hydrophilic acrylic, hydrophobic acrylic, and silicone intraocular lenses in eyes with uveitis having cataract surgery: Long-term follow-up. *J Cataract Refract Surg* **37**, 104–12 (2011).

[72] Aran, K., Sasso, L. A., Kamdar, N. & Zahn, J. D. Irreversible, direct bonding of nanoporous polymer membranes to pdms or glass microdevices. *Lab Chip* **10**, 548–552 (2010).

[73] KAPUSCINSKI, J. Dapi - a dna- specific fluorescent-probe. *Biotech. Histochem.* **70**, 220–233 (1995).

[74] Patterson, G. H. & Lippincott-Schwartz, J. A photoactivatable gfp for selective photolabeling of proteins and cells. *Science* **297**, 1873–1877 (2002).

[75] Reungpatthanaphong, P., Dechsupa, S., Meesungnoen, J., Loetchutinat, C. & Mankhetkorn, S. Rhodamine b as a mitochondrial probe for measurement and monitoring of mitochondrial membrane potential in drug-sensitive and -resistant cells. *J Biochem Biophys Methods* **57**, 1–16 (2003).

[76] Farnsworth, N., Bensard, C. & Bryant, S. J. The role of the pcm in reducing oxidative stress induced by radical initiated photoencapsulation of chondrocytes in poly(ethylene glycol) hydrogels. *Osteoarthritis Cartilage* **20**, 1326–35 (2012).

[77] Sriram, G. *et al.* Full-thickness human skin-on-chip with enhanced epidermal morphogenesis and barrier function. *Materials Today* –. URL https://www.sciencedirect.com/science/article/pii/S1369702117304844.

[78] Cartwright, L. *et al.* In vitro placental model optimization for nanoparticle transport studies. *Int. J. Nanomed.* **7**, 497–510 (2012).

[79] Correia Carreira, S., Cartwright, L., Mathiesen, L., Knudsen, L. E. & Saunders, M. Studying placental transfer of highly purified non-dioxin-like pcbs in two models of the placental barrier. *Placenta* **32**, 283–91 (2011).

Protocols

A Materials & manufacturing

A.1 3D printing

Materials:

- **.stl file by FreeCAD**
- **Software Slic3er by prusa**
- **Filament PLA**

Procedure:

1. drag and drop .stl file in Slic3er Software
2. check settings according to:

(a)

(b)
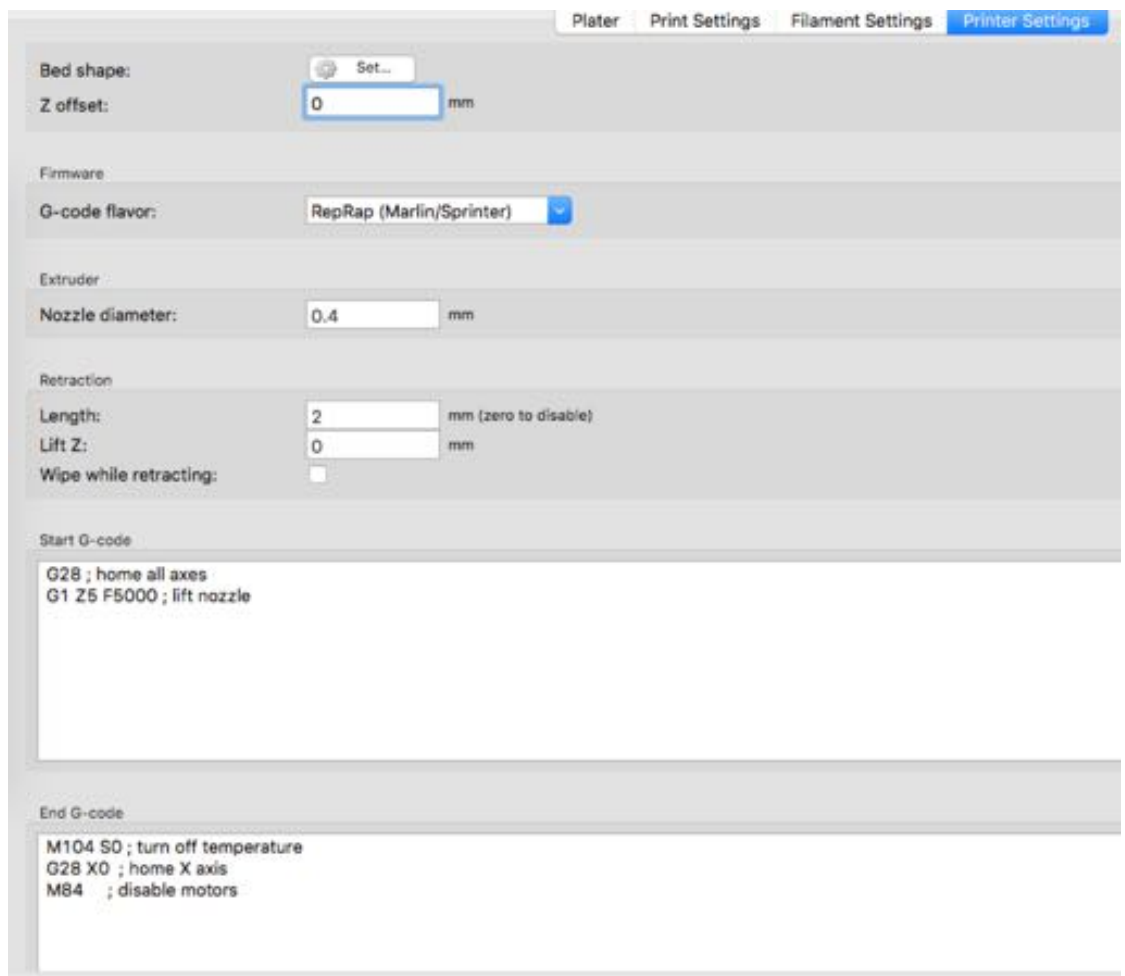
3. export to g-code file

4. save g-code file on printers SD card

5. run calibration file on printer (print from SD)

6. run your own file

A.2 Washing glasses

Materials:

- **glasses which needs to be washed**
- **Hellmanex III 2% solution in Water**
- **Isopropanol**
- **Water**

Procedure:

1. briefly wash **glasses** under running water

2. wash **glasses** by ultra sound with **Hellmanex** 2% solution for 5 min @ room temperature

3. briefly wash **glasses** under running water

4. wash **glasses** by ultra sound with **isopropanol** for 5 min @ room temperature

5. briefly wash **glasses** under running water

6. wash **glasses** by ultra sound with **water** for 5 min @ room temperature

A.3   Plotting foils (PDMS, ARcare, Sandblast foil)

Materials:

- **foil**

- **corresponding blade:**

  - PDMS foil // ARcare adhesive tape: **Roland ZEC-U5032** (yellow) for fluorescent and reflective film and vinyl film
  - sandblast foil: Roland **ZEC-U1715** (green) for sandblast stencil

Procedure:

1. mount foil in plotter and meassure size by plotter (2x down // SIZE with enter)

2. copy and paste design from Autocad in Roland Cut studio and adjust size (proberties with right click)

3. set cutting seetings (get size from machine)

4. values for materials:

   (a) **sandbalst foil**: cutting force 100 gf // cutting speed 20 cm/s // off set 0.25 // cutting quality HEAVY

   (b) **PDMS:** cutting force 80 gf // cutting speed 20 cm/s // off set 0.25 // cutting quality HEAVY

   (c) **ARcare 92712**: cutting force 80 gf // cutting speed 20 cm/s // off set 0.25 // cutting quality HEAVY (can be used with bladed liftet for ARcare 90106 and ARseal 90880)

   (d) **ARcare 90455**: cutting force 80 gf // cutting speed 20 cm/s // off set 0.25 // cutting quality HEAVY (can be used with bladed liftet for ARcare 90106 and ARseal 90880)

   (e) **ARcare 90106**: cutting force 100 gf // cutting speed 20 cm/s // off set 0.25 // cutting quality HEAVY

   (f) **ARseal 90880**: cutting force 100 gf // cutting speed 20 cm/s // off set 0.25 // cutting quality HEAVY

5. cut, unmount carefully and remove unneeded structure by tweezer

A.4 Powder blasting glass

Materials:

- **sandblast foil**

- **glass**

Procedure:

1. create mask according to protocoll A.3

2. stick it on top of the glass (to have a better result another mask can be placed on the back of the glass as well)

3. powder blast with Edelkorund F120 with 3 bar and with a distance of approx. 3cm between mask and nozzle

4. remove foil

5. wash glasses (see A.2)

A.5 Bonding PDMS to glass

Materials:

- **PDMS**

- **glass**

Procedure:

1. wash glass according to washing glassesA.2

2. activate surface by plasma oven for *1 min* at HIGH intensity

3. press glas and PDMS together manual

4. repeat step 1 and 2 for several layers

5. squezze struckture with clamps *over night* in oven at 70º C

A.6 Sample preparation for force testing

Materials:

- **glass slides**

- **tape to test**

- **press**

Procedure:

1. wash glasses

2. plott circles with area = 1 cmˆ2

3. bond with 250 N for 1 min between PDMS foil 250 µm

4. apply force with aprox. 10 N/sec for testing

A.7 Cutting optimization for Roland CAMM-1 Servo GX-24

Materials:

- **new blade depending on the material:**

  - PDMS foil // ARcare adhesive tape: **Roland ZEC-U5032** (yellow) for fluorescent and reflective film and vinyl film
  - sandblast foil: Roland **ZEC-U1715** (green) for sandblast stencil

- **material to be cut**

Procedure:
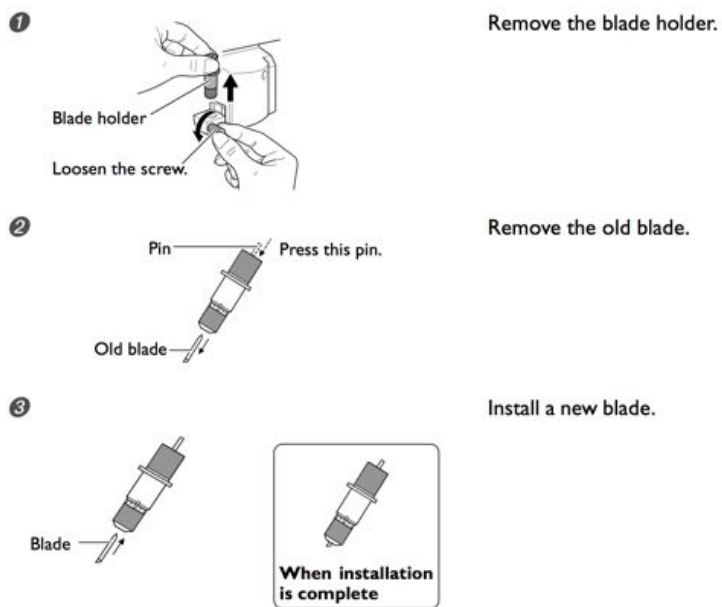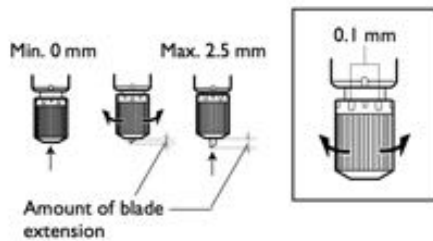
1. remove blade holder, remove old blade and install new blade

Figure 28: installing a new blade

2. adjust the blade extension

Adjusting the Cutting-in Amount

Min. 0 mm   Max. 2.5 mm   0.1 mm

Amount of blade extension

When you want to perform accurate and fine adjustment of the cutting-in amount, such as when cutting media with thin carrier paper, you can obtain good results by adjusting the tip of the blade.

Turn the cap portion of the blade holder to adjust the amount of blade extension.

A change in extension of 0.5 mm can be made by rotating the cap one full turn.

Rough Estimate for the Amount of Blade Extension

Use the following dimension as a rough estimate for setting the amount of blade extension.

$$\text{Amount of blade extension} = \text{Thickness of the media portion} + \frac{\text{Thickness of the carrier paper}}{2}$$

Material portion — Holder
Half of the carrier paper
Carrier-paper portion
Blade
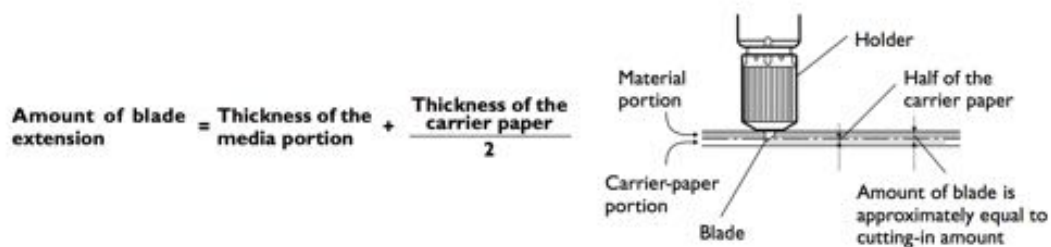Amount of blade is approximately equal to cutting-in amount

Figure 29: adjusting cutting in-amount

(a) first adjust blade extension to zero by eye and make at test scratch on paper to feel if the blade is still scratching the paper (it should be if you lift the blade for only a few µm if not it is at point zero)

(b) now adjust from zero the blade to the needed hight as described aboved: example if the carrier material on top has 100 µm the material 300 µm and the bottom carrier material 100 µm the blade has to be liftet by 450 µm (trun the cap by 324º)

(c) blade extension values for materials:

    i. **sandbalst foil**: 600 µm
    ii. **ARcare 92712**: 125 µm
    iii. **ARcare 90455**: 160 µm
    iv. **ARcare 90106**: 220 µm
    v. **ARSeal 90880**: 220 µm

3. put the blade back into the plotter

Support the screw from below and insert the blade holder.
If installed without supporting the screw in this way, cutting quality may become poor.

Insert until the collar is flush with the surface.
Screw
Support it from below.

Tighten the screw.
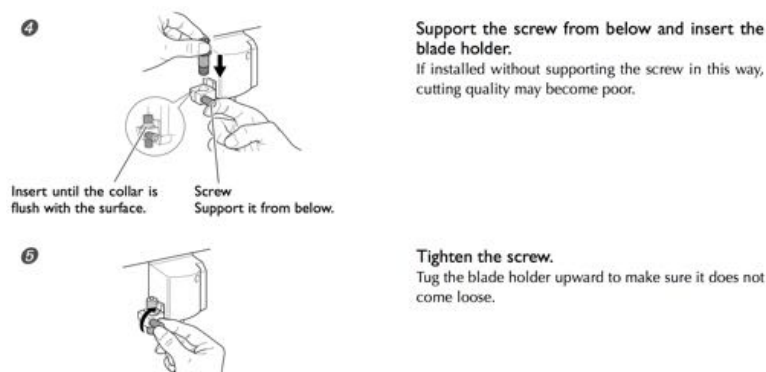Tug the blade holder upward to make sure it does not come loose.

Figure 30: blade holder fixation

4. make a test cut and ensure that the bottom carrier material is scratched which means that the top carrier material and the material is totally cut if not just level the blade by ca. 25 µm

5. Figure out the optimal blade force:

   (a) start with default settings: cutting force 80 gf // cutting speed 20 cm/s // off set 0.25 // cutting quality HEAVY

   (b) increase the force step wise and check if needed structure can be peeled of easily

   (c) values for materials:

       i. **sandbalst foil**: cutting force 100 gf // cutting speed 20 cm/s // off set 0.25 // cutting quality HEAVY

       ii. **ARcare 92712**: cutting force 80 gf // cutting speed 20 cm/s // off set 0.25 // cutting quality HEAVY (can be used with bladed liftet for ARcare 90106 and ARseal 90880)

       iii. **ARcare 90455**: cutting force 80 gf // cutting speed 20 cm/s // off set 0.25 // cutting quality HEAVY (can be used with bladed liftet for ARcare 90106 and ARseal 90880)

       iv. **ARcare 90106**: cutting force 100 gf // cutting speed 20 cm/s // off set 0.25 // cutting quality HEAVY

       v. **ARSeal 90880**: cutting force 100 gf // cutting speed 20 cm/s // off set 0.25 // cutting quality HEAVY

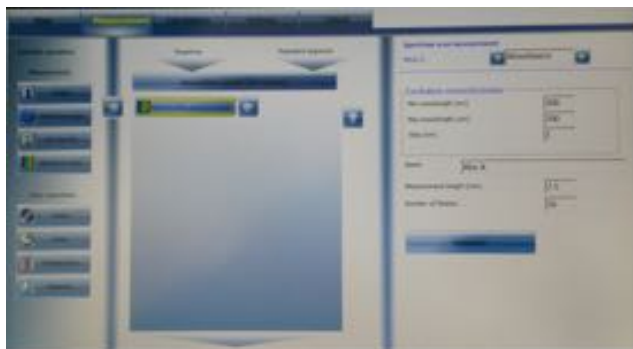## A.8 TEER chip production

Materials:

- **glasss with integrated electrodes**

- **sand blast foil**

- **membrane**

- **ARcare 90445**

Procedure:

1. create glass slides with channels according to A.4

2. powder plast holes (2 mm) for ports with same procedure but no washing because of electrodes

3. clean glasses with electrodes under running water

4. bath them in 50 mM FeCl3 for 40 sec. and clean them in DI water

5. punsh hole in membrane by biopsy puncher (1,5 mm)

6. prepare ARcare 90445 for channels according to A.3 and ARcare 90106 as sealing material

7. build ship from bottom to top (glass with electrodes (electrodes up!!!), ARcare 90445 with channel structure, glass with channel structure.....)

8. membrane can be placed on a sheet of PDMS foil in advance to ease the alignment

9. press chip carefully manual in the end to ensure bonding
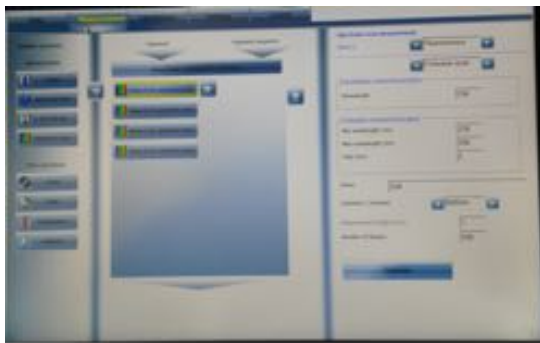
A.9   Absorption

Materials:

- **enspire 2300**

A.10 Emission

Materials:

- **enspire 2300**

68

B Cell culturing

B.1 Cell medium exchange

Materials:

- **Culture medium:** 5 ml (for T25 flask); 10 ml (for T75 flask)
- **PBS:** 5 ml

Procedure:

1. Drain old culture medium with suction pump
2. Add 5 ml of **PBS** and shake carefully to distribute well
3. Drain PBS
4. Add 5 ml (10 ml) of **culture medium**

B.2 Cell splitting

Materials:

- **Culture medium:** 5 ml + 9 ml (for T25 flask); 10 ml + 9 ml (for T75 flask)
- **PBS:** 10 ml
- **Trypsin:** 2 ml

Procedure:

1. Drain old culture medium with suction pump
2. Add 5 ml of **PBS** and shake carefully to distribute well
3. Drain **PBS**
4. Add 5 ml of **PBS** and shake carefully to distribute well
5. Drain **PBS**
6. Add 2 ml of **Trypsin** and shake carefully to distribute well
7. Put the Flask in the incubator for at least *10 min*
8. Add 4 ml of **Culture medium**, suck everything off with pipette and add in a 10 ml falcon tube
9. Put the tube in the centrifuge for *5 min* with 1100 rpm (140 rcf)
10. prepare new flask with c**ell culture medium**: 5 ml for T25 flask; 10 ml for T75 flask
11. Drain carefully old **culture medium** and **trypsin** by sliding the suction pump tip underneath the cell clump
12. dilute cell clump with 1 ml **culture medium** by pipetting several times
13. add **culture medium** according to split ration (e.g. add 4 ml of **medium** for spliting by 1:4)
14. put 1 ml of cell with **culture medium** into the prepared flask

B.3 Cell counting

Materials:

- **Culture medium:** 5 ml
- **Counting glass** with **cover glass**
- **Trypsin:** 1 ml
- **Trypsan Blue Solutio:** 10 µl

Procedure:

1. Proceed as described in protocol cell splitting (Appendices B.2) until centrifuging
2. Remove the medium
3. Add approx. 1 ml of medium and dilute cell palett by 1ml pipette
4. Add 3 ml of medium
5. Pipett 10µm into an eppi and add 10 µl of Trypsan Blue Solution (TBS)
6. Wet each outer area wirh 70% Ethanols to position the cover glass
7. fill the middle area with the mixture of medium and TBS
8. Use the microscope to count the number of cells block wise
9. Count four blocks calculate the cells/block
10. After that calculate number of cells/ml $= 20000 *$ number of cells/block (because of adding 10µl TBS)
11. Now separate the cells as wished

B.4 Freezing cells

Materials (for confluent T75 - 1/3 T75 = 1 ml forzen cell dispension):

- **DMSO:** 300 µl
- **FCS/FBS:** 300 ml
- **culture medium:** 3 ml

Procedure:

1. Proceed as described in protocol cell splitting (Appendices B.2) until centrifuging
2. Remove the medium
3. Add 3 ml of medium and dilute cell palett by 1ml pipette
4. Add 300 µl **DMSO** (10% of medium) and 300 µl **FCS/FBS** (10% of medium)
5. alliquote 1 ml of dispension
6. freez for at least 4h in styropor container @ - 80º C
7. store afterwards in liquid nitrogen

B.5 Cell seeding in chip

Materials:

- **Ethanol 70%:** 5 ml

- **PBS:** 5 ml

- **Collagen Type I from rat tail:** ca. amount of channel (http://www.sigmaaldrich.com/catalog/product/sigma/c38

- **HEPES:** 1% of medium needed (http://www.amresco-inc.com/STERILE-HEPES-1M-PH-7.3-J848.cmsx)

- **culture medium:** 5 ml

Procedure:

1. Flush chip with **ethanol**, fill channels with ethanol and wait untill all ethanol is evapoured (*ca. 45 min*)

2. Flush chip with **PBS**

3. Fill channel with membrane with **collagen** and let it rest for *30 min*

4. Add 1% **HEPES** to the needed amount of **cell culture medium**

5. Flush chip with **medium** and fill channels with **medium**

6. suck channels empty

7. Fill channel with the cell dispension for seeding (with HEPES)

8. exchange medium with HEPES every 2 days or perfuse chip

B.6 Life dead cell staining

Materials:

- **Calcein AM:** 2µl per ml (https://www.thermofisher.com/order/catalog/product/C3100MP)

- **Ethidium Homodimer-1 (EthD-1):** 4µl per ml (https://www.thermofisher.com/order/catalog/product/E1169)

- **Cell culture medium:** 1 ml

- additional 1µl per ml of medium Höchst per ml for blue staining of all cells

Procedure:

1. First check how much staining is needed: you need 1 ml for 1ml medium in culture (1:1)

2. Pipette needed amount of **Calcein AM** and **EthD-1** into a 15 ml Falcon tube

3. Add needed amount of **Cell culture medium** and mix it well

4. Add solution in ration 1:1 to the cells which need to be stained (Ex. cells are cultured in 1 ml medium add 1 ml soultuion) and mix it carefully

5. Incubate for *30 min*

Microscope:

1. For life staining (**Calcein AM**) use filter 2 (blue light) to see green living cells

2. For dead staining (**EthD-1**) use filter 3 (green light) to see red dead cells

B.7 Viability cell staining

Materials:

- **PrestoBlue:** 10% of cell culture medium (https://www.thermofisher.com/order/catalog/product/A13261?ICID=cv prestoblue-c1t1)

Procedure:

1. Add 10% **PrestoBlue** to the cell in medium (Ex. 50 µl PrestoBlue for 500 µl cell medium)

2. Mix it carefully

3. Incubate for *30 min*

Plate Reader EnSpire 2300:

1. use 96 well plate

2. pipett 100 µl of each sample into a well

3. use seba Presti 96 well protocoll to run viability quantification (take 50 - 100 flashes)
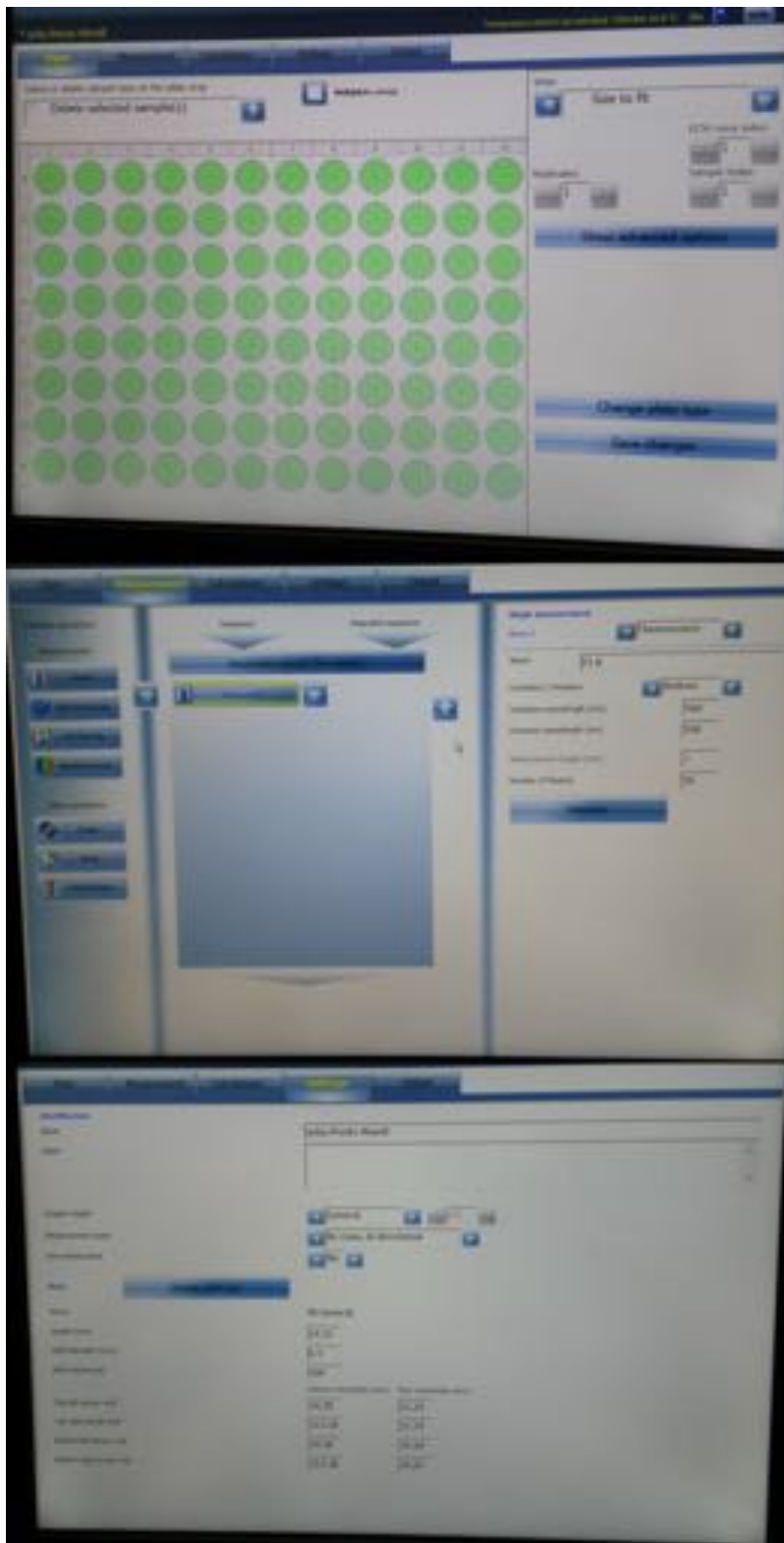
Figure 31: seba Presto 96 well protocoll